

ENGINEERING RESEARCH INSTITUTE
THE UNIVERSITY OF MICHIGAN
ANN ARBOR

SUMMARY REPORT ON THE STUDY OF THE FLOW OF PASTE

Seymour Calvert
Robert H. Miller
Alberto Molini
Nallam S. Chari

Project 2396

ATOMIC POWER DEVELOPMENT ASSOCIATES, INC.
DETROIT, MICHIGAN

November 1956

engm

UMR1050

TABLE OF CONTENTS

	Page
LIST OF FIGURES	iii
ABSTRACT	vii
OBJECTIVE	vii
INTRODUCTION	1
OBJECTIVES OF RESEARCH SINCE JANUARY, 1956	4
SUMMARY	5
1. LITERATURE SEARCH	5
2. HAIRPIN FLOW	5
3. FLOW THROUGH ORIFICES	5
4. COEFFICIENT OF FRICTION MEASUREMENTS	6
5. EXPLORATORY DOWNWARD AND HORIZONTAL FLOW SYSTEMS	6
6. COMPLETE REACTOR FLOW SYSTEMS	6
RESEARCH RESULTS	6
LITERATURE SEARCH	7
HAIRPIN SYSTEMS	7
FLOW OF PASTE THROUGH ORIFICES	15
COEFFICIENT OF FRICTION	23
EXPLORATORY EXPERIMENTS ON DOWNWARD AND HORIZONTAL FLOW SYSTEMS	26
COMPLETE REACTOR FLOW SYSTEMS	27
REFERENCES	30

LIST OF FIGURES

Figure		Page
1	Hairpin exits.	8
2	Solids flow rate versus pressure drop for upward flow of glass beads in a 10.3-mm-ID hairpin with overflow exit.	31
3	Total flow rate versus pressure drop for upward flow of glass beads in a 10.3-mm-ID, 2-ft-long hairpin with overflow exit.	32
4	Total flow rate versus pressure gradient for the downward flow of glass beads in a 10.3-mm-ID hairpin with overflow exit.	33
5	Total flow rate versus pressure drop for downward flow of glass beads in a 10.3-mm-ID hairpin with various exit types.	34
6	Pressure drop versus flow rate for downward flow of 82-micron Ottawa sand in a 10.2-mm-ID, 2-ft-long hairpin with overflow exit.	35
7	Pressure drop versus flow rate for downward flow of 82-micron Ottawa sand in a 10.2-mm-ID, 4-ft-long hairpin with overflow exit.	36
8	Pressure drop versus flow rate for downward flow of 98-micron Ottawa sand in a 10.2-mm-ID, 2-ft-long hairpin with overflow exit.	37
9	Total flow rate versus solid flow rate for upward flow of Ottawa sand in a 10.2-mm-ID hairpin with overflow exit.	38
10	Total flow rate versus solid flow rate for upward flow of copper shot in a 10.3-mm-ID hairpin with overflow exit.	39
11	Total flow rate versus solid flow rate for upward flow of 100/120-mesh glass beads in a 10.3-mm-ID tube with various exit types.	40

LIST OF FIGURES (Cont.)

Figure		Page
12	Paste velocity versus pressure drop for downward flow of Ottawa sand in a 17.8-mm-ID, 4-ft-long hairpin with overflow exit.	41
13	Paste velocity versus pressure drop for upward flow of Ottawa sand in a 17.8-mm-ID, 4-ft-long hairpin with overflow exit.	42
14	Volume fraction solids versus paste flow rate for 100/140-mesh Ottawa sand in a 17.8-mm-ID hairpin with plain- and washed-overflow exits.	43
15	Total flow rate versus solids flow rate for upward flow of 100/140-mesh Ottawa sand in a 17.8-mm-ID hairpin with washed exit.	44
16	Flow rates versus pressure drop for downward flow of 100/140-mesh Ottawa sand in a 17.8-mm-ID hairpin with washed exit.	45
17	Volume fraction solids versus solids flow rate for upward flow of 100/140-mesh Ottawa sand in 8-mm-ID and 17.8-mm-ID tubes. Porosity determined by electrical conductivity method.	46
18	Total flow rate versus solids flow rate for upward flow of 100/120-mesh glass beads in an 8-mm-ID hairpin with washed exit.	47
19	Predicted free water velocity versus particle diameter with volume fraction solids as parameter for spheres with density of 2.49 gm/cm ³ flowing upward at $R_{OW} = 1$.	48
20	Predicted free water velocity versus particle diameter with volume fraction solids as parameter for spheres and "round sand" with density of 2.65 gm/cm ³ flowing upward at $R_{OW} = 1$.	49
21	Predicted free water velocity versus particle diameter with volume fraction solids as parameter for spheres with density of 8.65 flowing upward at $R_{OW} = 1$.	50
22	Predicted free water velocity versus particle density with particle diameter as parameter for upward flow of spheres at $R_{OW} = 1$ and $(1-X) = 0.55$.	51

LIST OF FIGURES (Cont.)

Figure		Page
23	Predicted free water velocity versus particle density with particle diameter as parameter for upward flow of "round sand" at $R_{ow} = 1$ and $(1-X) = 0.55$.	52
24	Sketch of equipment.	53
25	Pressure drop versus solids flow rate with orifice diameter as parameter for the flow of 80/100-mesh Ottawa sand paste.	54
26	Pressure drop versus solids flow rate with orifice diameter as parameter for the flow of 140/200-mesh Ottawa sand paste.	55
27	Pressure drop versus solids flow rate with orifice diameter as parameter for the flow of 200/325-mesh Ottawa sand paste.	56
28	Pressure drop versus solids flow rate with orifice diameter as parameter for the flow of 140/200-mesh copper shot.	57
29	Pressure drop versus solids flow rate with orifice diameter as parameter for the flow of 140/200-mesh lead shot.	58
30	Logarithm of the slope function versus reciprocal of orifice diameter.	59
31	C_2 versus particle diameter.	60
32	C_1 versus reciprocal of particle density.	61
33	Coefficient of friction between a zinc plate and 150/200-mesh Ottawa sand paste.	62
34	Coefficient of friction between a glass plate and 150/200-mesh Ottawa sand paste.	63
35	Coefficient of friction between a glass plate and -325-mesh iron-powder paste.	64
36	Viscometer apparatus sketch.	65
37	Viscometer torque versus fraction solids for 100/140-mesh Ottawa sand.	66
38	Viscometer torque versus fraction solids for 100/140-mesh copper shot.	67

LIST OF FIGURES (Concl.)

Figure		Page
39	Viscometer torque versus fraction solids for 100/120-mesh glass beads.	68
40a	Complete reactor configuration.	69
40b	Experimental model configuration.	69
41	Reactor top and bottom configurations.	70

ABSTRACT

A thorough survey of the literature yielded little worth-while information. Work on hairpin-type systems has been completed and a correlation of liquid and solid flow rates and pressure drop is presented. The special significance of small restrictive force at the tube exit is discussed. Work on nonflow systems intended to determine the frictional properties of pastes is described and the results are shown to agree with flow-experiment results. Data and a tentative correlation for flow through orifices are presented. The correlation includes particle diameter and density, orifice diameter, pressure drop across the orifice, and flow rates. Exploratory work on horizontal and multiple-hairpin downward flow is discussed. Design concepts for a complete reactor system and an experimental model are discussed.

OBJECTIVE

The object of this study is to establish a generalized correlation of the variables involved in the flow of high-density sediments through tubes. This will include experimental and analytical studies of both flow through tubes alone and complete, continuous flow loops.

INTRODUCTION

This report covers the work done during the period from January, 1956, to September, 1956, on a study of the flow of pastes. The study which began in June, 1955, had its origin in the desire of the Atomic Power Development Associates to investigate the feasibility of using a paste fuel composed of uranium (or uranium compound) particles in liquid sodium. This application requires that the paste have a high density (solids content) and that it move at extremely low velocity.

Because of these requirements we are concerned with a type of flow which has received practically no study in the past. Considerable information is available on the flow of suspensions, but this is not applicable here because it does not cover systems where force may be transmitted independently through particle-to-particle contact. As has been learned in this study, this mechanism of force transmission can produce profoundly distinct effects. This brief explanation points out the underlying factors which required that much of the study be exploratory.

The first step in the study was to learn whether the paste would flow at all at the density desired. Next came the determination of what variations of flow parameters were possible and, following that, what the order-of-magnitude force relationships were for the flow. This ground was covered in the work performed prior to the first of this year, although there were still lessons to be learned on the nature of the significant variables. The first three months' work was reported in Summary Report on a Preliminary Study of the Flow of Paste, September, 1955. Its nature is shown in the following excerpts from that report.

"Subject.—The determination of the pressure-drop—flow-rate relationships for the flow of high-density pastes through tubes is required for the estimation of design requirements of a reactor. The system contemplated would have the following characteristics:

1. Paste is composed of uranium oxide or uranium powder suspended in molten sodium or sodium potassium.

- a. Density should be at least 40-50 volume-percent solids.
- b. Particle size may be varied to obtain optimum flow character-

istics. A size range around 50-micron diameter is envisioned.

2. Tube diameter will be in the range of 1/4 to 1 in. Tube material will be stainless steel, probably 304.
3. Flow rate is anticipated to be in the range of 1/3 to 10 ft per day.
4. The orientation of the tube may range from horizontal to vertical.

"Object.—The object of this preliminary study is to obtain order-of-magnitude data on the pressure drop required to produce the desired flow rate and some insight into the mechanism of flow.

"For highly concentrated suspensions such as those of present interest, there are four general possibilities for the type of flow. If there is no appreciable attraction between the particles, there are two possibilities: the suspension will flow as a viscous fluid whose viscosity depends only on solids concentration and particle-size distribution, or the suspension may be so concentrated that it must increase in volume when sheared (i.e., it is dilatant). If there is attraction between particles, then the third possibility will occur and the behavior will be non-Newtonian and will exhibit a yield stress.

"The fourth possibility, which is dependent on the methods of feeding and withdrawal, is that the liquid could flow at a different linear velocity than the solid.

"Because of the range of possible modes of flow and the lack of generalized information which would enable the prediction of flow characteristics, it will be necessary to conduct an experimental study.

"The variables to be investigated as time permits are:

1. Flow rate
2. Paste density
3. Particle-size and size distribution
4. Tube material and wall finish
5. Tube geometry - turns and fittings
6. Vibration of the tube and/or pulsation of the pressure.

"In view of the exploratory nature of this work, its course was discussed frequently in meetings with A.P.D.A. personnel, Dr. McDaniel, Mr. R. Thomas, and Mr. L. Kintner. These discussions made it possible to direct our efforts to the most significant points in the overall problem of determining the feasibility of the proposed system as the picture gradually took shape in the light of each new finding.

SUMMARY

"The key fact disclosed by this study is that the mechanism of flow corresponds to the fourth possibility suggested above. The solids settle to a bed of about 61 to 62 volume-percent solids which will move under the influence of fluid passing through it. If, on the other hand, the motive force bears directly upon the solid particles, as when a piston is used for pushing, the bed cannot be moved if its length is more than about 2-1/2 tube diameters. Measurements of shear stress versus rate of shear with a concentric-cylinder viscometer are not directly applicable to flowing systems since the shear stress (or friction) depends on the bearing force exerted by the weight of the solids on the rotating cylinder. In fact, the rotating cylinder can be stopped by pressing with a finger on top of the sand surrounding the cylinder.

"Once it was demonstrated that force was transmitted through the continuous sediment of particles as well as through the fluid, it became apparent that our previous knowledge of the flow of suspensions was not applicable. Our attention was then directed to the study of the flow of fluids through moving porous beds. Most of this work was done with water and silica flowing through glass tubes. Exploratory experiments with glass beads and copper metal powder indicated the same type of behavior as is exhibited by the silica. Flow through horizontal runs generally exhibits stratification with most of the water flowing in the upper 1/4 of the tube. Consequently, attention was centered on vertical upward and downward flow."

The work for the next four months had substantially the same objective and was reported in Summary Report on Continuation of the Study of the Flow of Paste, January, 1956. The summary of that work was presented in the report as follows:

SUMMARY

"The work performed during this four-month period was in five areas:

1. Construction of apparatus and obtaining data on paste flow in vertical hairpins up to 8 ft in length (16 ft of tube length). All the data, except one run on copper powder, are for rounded or angular silica particles. There are not yet sufficient data to permit any quantitative generalizations.

2. Construction of apparatus and obtaining data on the pressure drop required for fixed-bed expansion. The data show the inapplicability of the point of first expansion as a criterion of frictional effects. The points of

maximum and equilibrium pressure drop seem promising as criteria.

3. Investigation of the applicability of electrical-conductivity measurement as a means of determining bed porosity. The method appears to be satisfactory and will be used in future work.

4. A literature search. No applicable information was found in the areas and time period covered.

5. Design conception and exploratory experimentation on continuous-flow loop systems. A system incorporating downward flow of dense paste inside a tube and low-density left for solids recycle was operated satisfactorily on sand and water. Examples of various conceivable system types are discussed."

OBJECTIVES OF RESEARCH SINCE JANUARY, 1956

The work reported here began in January, 1956, and its scope was set forth in a proposal for a continuation of the study as follows:

Object: The object of this study is to establish a generalized correlation of the variables involved in the flow of high-density sediments through tubes. This will include experimental and analytical studies of both flow through tubes alone and complete, continuous flow loops. The variables to be investigated are:

- Scope:
1. Flow parameters
 - a. Paste rate - 0 to 30 ft/day.
 - b. Liquid rate - as required to give desired paste flow rate.
 - c. Paste density.
 2. Particle parameters
 - a. Size and size distribution - concentrate on size distribution like that of actual fuel particles. Mixtures will run from 44 to 200 microns with a 100 micron median size.
 - b. Density - cover as wide a range as possible.
 - c. Shape - Rounded and angular parameters.
 3. Tube
 - a. Cross-section - Round and rectangular.
 - b. Diameter - 1/4" to 1".
 - c. Length - up to 20 ft total.
 - d. Geometry - Straight downward sections, single hairpins, and multiple hairpins.
 - e. Material and surface finish.

4. Effect of geometries such as manifolds, contractions, and turns.
5. Effect of all components and controls required for continuous flow loop operation.

Method: The method of approach to the problem will be as follows:

1. Complete the literature search.
2. Conduct experiments on flow systems.
3. Conduct such experiments on non-flow systems as will yield information on the characteristics of the paste which may be correlated with behavior in flow systems.
4. Analyze and correlate the data.
5. Apply the correlations to a representative design or designs for a paste flow reactor system."

SUMMARY

The results of the work performed during this period are summarized as follows:

1. LITERATURE SEARCH

The literature search has been completed and the result confirms our preliminary finding that no significant information is available.

2. HAIRPIN FLOW

Following a period of considerable difficulty in obtaining data on hairpins with 180° exit bends and overflow-type exits, it was discovered that washing the particles away from an overflow exit results in flow at a constant pressure drop in the upward leg. When the exit is washed or submerged, the pressure drop in the upward leg is always equivalent to the buoyant weight of the solids.

Data on 180° exit bends and unwashed overflow exits are now recognized as relating to special, incompletely defined cases in which some unknown force is applied to the particles at the exit. A mathematical analysis substantiates the validity of the conclusion from experimental data.

3. FLOW THROUGH ORIFICES

Work, which is still in progress, on the flow of paste through

orifices yielded data showing a clear relationship between flow rates and pressure difference across the orifice, orifice diameter, and particle diameter. The data are not yet sufficient to permit a correlation of all variables.

4. COEFFICIENT OF FRICTION MEASUREMENTS

The coefficient of friction as a function of bed density was determined by means of a loaded sled apparatus and is shown to decrease at a critical density. Friction between a rotating cylinder and beds of particles with water flowing upward through the bed has been measured. In this case there is also a change in friction at about the same bed density as for the sled measurements.

5. EXPLORATORY DOWNWARD AND HORIZONTAL FLOW SYSTEMS

It was discovered that downward and horizontal flow without stratification may be obtained if the tube exit is restricted. The ratio of solids flow rate to liquid flow rate required to make the tube run full of solids is maintained because of the exit-orifice characteristics.

6. COMPLETE REACTOR FLOW SYSTEMS

Consideration of the requirements of the complete reactor system has resulted in the formation of several concepts of top and bottom paste distribution and collection schemes. An experimental model based on one such concept was built and preliminary experiments with it were inconclusive.

RESEARCH RESULTS

The nature and results of the research carried out during this period will be presented below. The major topic divisions are:

1. Literature search.
2. Hairpin systems.
3. Flow through orifices.
4. Coefficient-of-friction measurements.
5. Downward and horizontal flow systems.
6. Complete reactor flow systems.

LITERATURE SEARCH

A literature search covering the references in Chemical Abstracts back to 1927 disclosed no significant amount of background information. A large number of patents dealing with the flow of particulate material have been examined, but no worth-while data were found.

There are four references which deal with special cases of the paste-flow problem. These are as follows:

1. "Flow of Granular Material Through a Circular Orifice," F. C. Franklin and L. N. Johansen, Chem. Eng. Science, 4, 119 (1955).
2. "Forces Acting in Flowing Beds of Solids," J. W. Delaplaine, AIChE, 2, 127 (1956).
3. "Flow of Solid Particles Through Orifice," G. Kwai, Chem. Eng. (Japan), 18, 453 (1953).
4. "Discharge Rate of Solid Particles From a Nozzle Steeped in Liquid," Y. Oyama and K. Nagano, Repts. Sci. Research Inst. (Japan), 29, 349 (1953).

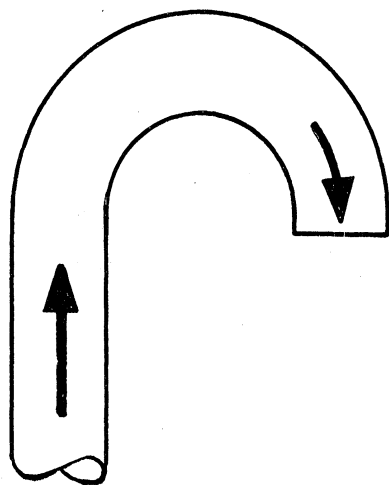
The first three references deal with the flow of dry particles and the last with the flow of particles and water with a constant head of water above the orifice. A comparison of these data with the experimental results of this program is presented in a later section of this report.

HAIRPIN SYSTEMS

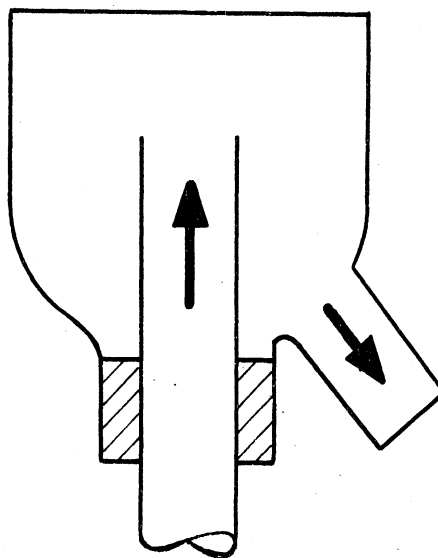
The previously initiated study of flow through vertical hairpin tubes was extended to cover a wider range of variables. It was intended that continuous-flow, automatically controlled systems be used for this work, but it was not possible to find liquid controls suitable for such low flow rates. Consequently, the apparatus was the same as that used previously, that is, it involved a batch-loaded solids reservoir and water rate was adjusted manually.

After a period of considerable difficulty in obtaining reproducible data and steady-state conditions within a working day, the exit configuration was changed. Since it was suspected that the 180° bend was exerting force on the particles, an overflow-type exit was introduced. The configuration of this exit is shown in Fig. 1. With the overflow exit the data were still erratic and did not check the data obtained with the 180°-bend exit.

Finally it was discovered that the small mound of particles which built up on the tube exit had a profound effect on the pressure drop. A small



180°-RETURN-BEND
EXIT



OVERFLOW EXIT

Fig. 1. Hairpin exits.

nozzle was placed above the tube exit so that the particles leaving the tube could be washed away and not pile up above the tube end. The remaining runs were made with the washed overflow exit.

A summary of the valid runs made since January, 1956, is presented in Table I.

The data for most of the runs listed in Table I are represented in Figs. 2 through 18. In cases where the data are for upward flow at an overweight ratio (R_{ow}) of 1.0, the plots show total flow rate versus solids flow rate as points and the predicted values (to be discussed later) as lines. No plots are given for runs 8 through 11 since the flush-water rates and thus total flow rates were not known accurately. These were the first runs in which the washed exit was used and their value lies in the fact that they show flow at an overweight ratio of 1.0.

Some of the runs with the washed exit indicated a decrease in flowing density with flow rate, as shown in Fig. 14. Upon further investigation it was found that the density in the upward leg remained constant at the loosely settled density at all flow rates once a high enough flow rate was attained. In other words, flow at a density higher than the loosely settled density is an unstable situation which can be eliminated by either "breaking-in" the system at a high flow rate or by letting it run for a long period.

TABLE I

SUMMARY OF HAIRPIN RUNS

Run	Figure	Tube Diameter (mm)	Tube Length (ft)	Particles	Exit	Upward Leg Overweight Ratio (approx.)
1	6-9	10	2	82 μ O.S.	overflow	1
2			2	98 μ O.S.	overflow	1
3			4	82 μ O.S.	overflow	1
4	12-16	18	4	100/140 O.S.	overflow	1.1-2.0
5			4	140/200 O.S.	overflow	1.1-2.0
6			4	-200 O.S.	overflow	1.1-2.0
7		18	4	100/140 O.S.	washed	1.0
8		8	10	100/120 G.B.	overflow	2-3
9		8	10	100/120 G.B.	washed	1.0
10		8	10	20/28 G.B.	washed	1.0
11		8	6	140/200 O.S.	washed	1.0
12	2-5	10	2	100/120 G.B.	overflow	2.0-4.0
13			2	170/200 G.B.	overflow	1.8-4.0
14			2	270/325 G.B.	overflow	1.3-8.5
15			2	16/20 G.B.	overflow	2.0-2.5
16			2	32/35 G.B.	overflow	2.2-2.8
17			2	80/100 G.B.	overflow	1.6-2.5
18			10	10	2	140/200 Cu
19	2	200/325 Cu			overflow	1.0
20	2	100/120 G.B.			notched overflow	1.0
21	11	10	2	100/120 G.B.	washed	1.0
22			2	100/120 G.B.	90° bend	1.0
23			2	100/120 G.B.	180° bend	1.0
24	11	18	2	100/120 G.B.	washed	1.0
25	15	18	2	100/140 O.S.	washed	1.0
26	11	18	2	100/120 G.B.	washed	1.0
27	15	18	2	100/140 O.S.	washed	1.0
28	18	8	2	100/120 G.B.	washed	1.0

Figure 17 shows this effect.

It is quite clear from the data shown here and from our prior data on 180° exit-bend systems that the only definable (or reproducible) system is the washed-exit type. In some cases a 180° exit bend will cause a high pressure drop and in others it gives the same result as a washed exit. The same can be seen for the plain overflow system. The essential difficulty is that the restraining force at the exit depends on the particular way in which particles pile up at the exit and this has not been consistent for the return bend and plain overflow exits.

Correlation of Data.—Once the nature of the upward flow system was known it became possible to describe its behavior. That is, we base the description on the following facts:

1. The washed-exit system is the basic upward flow situation with no restraining force on the particles at the exit.
2. Friction between the flowing paste and the tube wall is negligible in upward flow.
3. The paste flows at approximately its loosely settled density in the upward leg and at a higher density, approaching the tightly settled density, in the downward leg of a hairpin with washed exit.

We must add a further restriction that this correlation will apply only to systems of the hairpin type where the solids flow rate is not restricted. Another way of putting this is that this covers the case of minimum ratio of liquid rate to solid rate. This is to differentiate the high-density flow regime from the low-density regime in which for any solid rate there can be a range of liquid rates.

With the above restrictions, the only problem remaining is to find a relationship which will indicate the liquid flow rate required to exert drag on the particles equal to the weight of the particles. We found that the correlation by Leva et al.¹ for the laminar flow of fluids through porous media is satisfactory for this purpose. The method of correlation is as follows:

$$V_w = V_T - \frac{V_s}{(1-X)}, \quad (1)$$

where

V_w = free liquid velocity (cm³/min/cm²) (based on the total cross-sectional area of the tube),

V_T = total flow velocity (cm³/min/cm²),

V_s = dry-solids velocity (cm³/min/cm²), and

X = volume fraction voids in flowing paste.

Thus V_w is the liquid velocity relative to the moving paste based on the total tube cross section. It is this velocity which is related to the frictional pressure drop. Leva's correlation for the laminar flow of fluids through porous media is

$$\Delta P = \frac{200 G \mu L \lambda^2 (1-\delta)^2}{D_{pf}^2 \rho' g_c \delta^3} \quad (2)$$

for

$$Re = \left(\frac{D_p G}{\mu} \right) < 10,$$

where

ΔP = frictional pressure drop over bed (lb/ft²)

G = mass flow rate (lb/sec/ft²) (based on total cross-sectional area of tube),

μ = fluid viscosity (lb/ft/sec),

L = bed length (ft),

λ^2 = empirical shape factor which is 1.0 for spheres, 1.35 for round sand, and 2.25 for sharp sand,

δ = volume fraction voids,

D_{pf} = particle diameter (ft),

ρ' = fluid density (lb/ft³),

g_c = 32.2 (ft/sec²), and

Re = Reynolds number.

This relationship can be evaluated at the point where the pressure drop per unit length is equivalent to the buoyant density of the solid particles in the bed. After doing this and changing some of the variables to more comfortable units, we have

$$V_w = C_1 \frac{(\rho_s - \rho) D_p^2 X^3}{(1 - X)}, \quad (3)$$

where

C_1 = a constant depending on shape, and equal to $\left(\frac{2.94 \times 10^{-4}}{\lambda^2} \right)$,

ρ_s = density of dry solid (gm/cm³),

ρ = density of liquid (gm/cm³),

D_p = particle diameter in microns, and

$X = \delta$ = volume fraction voids.

Equation 3 is represented in graphical form in Figs. 19 through 23. In each of the first three figures free water rate is plotted against particle diameter with volume fraction solids as the parameter for a particular solid density. In the last two figures (22 and 23), free water rate is plotted against solid density with particle diameter as the parameter and for $(1-X) = 0.55$.

The value of $(1-X) = 0.55$ for average flowing density seems to be a fairly good approximation for rounded and spherical particles. Spherical particles such as glass beads exhibited flowing and loosely settled densities of about 57% solids while rounded sand ran about 55%. The loosely settled densities were determined in tubes of various diameters from 8 mm to about 30 mm and were not appreciably affected by tube diameter in this range. Since the effect of bed density is slight (see Figs. 19 through 21) in this range, this is not a crucial point.

Prediction of Flow Rates.—The application of the above correlation simply requires the determination of paste and free liquid flow rates for the upward flow of a particular solid and their addition to give total flow rate. Since the flowing density is constant, paste flow rate is a linear function of solid flow rate and is represented by a straight line going through the origin on Cartesian coordinates. Free liquid rate is a constant value if bed density is constant, so the line representing total flow rate lies parallel to the paste flow line and the intercept at $V_s = 0$ is the free liquid rate.

Discussion of Results.—The most significant result of this study was the realization of the overwhelming importance of small changes in the restraining force at the tube exit. By way of hindsight, this observation can be verified mathematically as follows.

Consider a differential element of paste in a vertical tube of radius r and represent the steady-state condition by a force balance across the element.

$$F + F_f + F_w - F_d - (F + dF) = 0 \quad (4)$$

and

$$dF = F_f + F_w - F_d,$$

where

F = force acting on particles in the downward direction,

F_f = force acting on particles due to wall friction,

F_w = force due to the weight of the particles,

F_d = force due to fluid drag on the particles, and

dF = increase in force across the element.

Then, assuming that wall friction is due to a normal component of "pressure" acting on the particles,

$$F_f = \frac{C_2 F (2\pi r)}{\pi r^2} \quad (5)$$

and

$$dF = \left[\frac{C_2 F (2\pi r)}{\pi r^2} - \left(\frac{\Delta P}{L} - \rho_b \right) \pi r^2 dL \right], \quad (6)$$

where

C_2 = a constant relating axial "pressure" to frictional force;

ΔP = frictional pressure drop across element due to fluid flow; in the strict sense this should be $-\Delta P$, but what is meant here is that a decrease in pressure in the upward direction corresponds to a positive ΔP ; this convention is employed to make the relationship between $\Delta P/L$ and ρ_b more clear;

ρ_b = buoyant bed density of particles; that is, particle density minus fluid density times volume fraction solids; and

L = bed length.

Integration of Equation 6 yields

$$\frac{r}{2C_2} \ln \left[\frac{2C_2 F}{r} - \left(\frac{\Delta P}{L} - \rho_b \right) \pi r^2 \right] = L + C_3. \quad (7)$$

At $L = 0$, $F = F_0$ = force at exit and

$$C_3 = \frac{r}{2C_2} \ln \left[\frac{2C_2 F_0}{r} - \left(\frac{\Delta P}{L} - \rho_b \right) \pi r^2 \right]. \quad (8)$$

Combining Equations 7 and 8 yields

$$2C_2 \frac{L}{r} = \ln \left[\frac{\frac{2C_2 F}{r} - \left(\frac{\Delta P}{L} - \rho_b \right) \pi r^2}{\frac{2C_2 F_0}{r} - \left(\frac{\Delta P}{L} - \rho_b \right) \pi r^2} \right]. \quad (9)$$

We now need to estimate "C₂," which is the product of the ratio of normal to axial particle-to-particle pressure times the coefficient of friction. This will be about 0.5 x 0.6 = 0.3. Equation 9 shows that even for a short tube of length = 20 radii the ratio of the numerator to the denominator on the right side of the equation is about 10⁸. Thus the difference between the two terms in the denominator must be extremely small or an impossibly large force will be exerted upon the solids at the bottom of the upward leg. That is,

$$\frac{2C_2F_0}{r} \approx \left(\frac{\Delta P}{L} - \rho_b \right) \pi r^2 \quad (10)$$

If we now assume that F₀ is due to a hemisphere of solids of radius r, sitting on top of the exit,

$$F_0 = \frac{4}{3} \pi r^3 \rho_b \quad (11)$$

Then, substituting in Equation 10,

$$\frac{(.6)1.33 \pi r^3 \rho_b}{r} = \left(\frac{\Delta P}{L} - \rho_b \right) \pi r^2 \quad (12)$$

and

$$\frac{\Delta P}{L} - \rho_b = .8 \rho_b \quad .$$

By definition,

$$R_{ow} = \frac{\frac{\Delta P}{L}}{\rho_b} \quad (13)$$

$$R_{ow} = \frac{1.8 \rho_b}{\rho_b} = 1.8 \quad (14)$$

Equation 14 indicates that the effect of a small restraining force at the exit of an upward leg can require an overweight ratio of considerably more than one. The variation in overweight ratio required for upward flow, as shown in Fig. 2, for example, can now be interpreted as being dependent on the ability of particles to remain in a distinct heap. The smaller the particles are, the more restrained they are by the surface tension of water, and the larger the mound at the exit can grow.

Flowing Density.—For the purpose of prediction in cases where there are no data on the actual material the values of 55% for upward flow density and 60% for downward flow density are adequate for rounded particles of fairly uniform diameter.

For cases in which there is a wide range of particle size or where the particles are angular, it would be best to determine the freely settled density experimentally. It is not possible to characterize flowing density as a function of flow rate alone, as is seen from the difference in upward and downward leg densities. The density is affected by force exerted on the particles at the tube exit, but we are unable to define this relationship from the data we have.

Prediction of Flow Rates.—As can be seen in Figs. 9, 10, 11, 15, 17, and 18, the predicted relationship is generally quite good for glass beads and copper shot, while it is less accurate for the Ottawa sand. The deviation between experimental data and prediction for the glass beads in the 8-mm tube (Fig. 18) is not understood and seems quite strange in view of the agreement obtained for the same beads in a 10.3-mm tube (Fig. 11).

From the standpoint of the objectives of this program it is not worth-while to pursue the subject of hairpin flow any further at this time. The correlation based on Leva's equation is sufficiently accurate for the purpose of engineering design and will make possible a fairly accurate estimate of energy requirements, etc., for a hairpin reactor system. Sufficient work has been done by previous investigators to indicate that the prospect of obtaining an extremely accurate general correlation for flow through porous media is quite dismal. If a hairpin system should appear advantageous at some future time (although it does not now), the next step would be to work with the actual solid particles in order to obtain more precise results.

FLOW OF PASTE THROUGH ORIFICES

In practically any paste-flow reactor system one can envision the use of an orifice at some point as necessary. Either the orifice will be used to restrain solids flow in the paste channel or it will be used to control the flow of solids into the low-density lift system. Since the prior knowledge of the flow of paste through orifices was very spotty and inadequate, it was necessary to perform an experimental study.

The method and results of this study are presented below, following a discussion of the literature. A tentative correlation of the data has been made, and while it is sufficiently accurate for engineering design estimates we are not satisfied with it and will modify it in the future as more data become available. It should also be emphasized that the system studied did not encompass a very wide range of geometric variations, so these results should be thought of as pertaining to a special case until we learn more about it.

Review of Literature.—A number of investigators have studied the mechanism of flow of solid particles being discharged through orifices. The

first to perform a thorough investigation of the factors influencing the flow of solid particles through orifices were Bingham and Wikoff.² They were trying to characterize some of the inherent properties of powders by means of simple free-flow gravity tests. Their work was of such a fundamental nature that a discussion of their results is very much indicated.

While for real liquids the effect of temperature upon the flow rates is of great importance, for solid particles it was found to be quite negligible. For real liquids, the head above the orifice would control the rate of discharge; however, with solid particles it was found that doubling the head did not increase the flow rates. On the contrary, higher heads caused lower discharges, supposedly due to denser packing near the orifices. The length of the capillaries was found to have a very important effect on the discharge rates. Larger flows were obtained with longer capillaries, especially when working with the finer particles. This was explained by the air-suction effect produced by the free fall of the particles.

Bingham and Wikoff² arrived at an empirical formula which expressed the discharge rates proportional to $D_o^{2.65}$, where D_o was the diameter of the capillary.

Wieghardt³ studied the discharge of sand from cylindrical vessels having a small hole at the bottom. Provided that the diameter and the height of the vessel were both sufficiently larger than the diameter of the hole, he found that the discharge rates were proportional to $D_o^{2.5}$, where D_o was the diameter of the orifice. This value for the exponent applies for orifices, not for capillaries.

Brown and Hawksley⁴ studied the flow patterns of a bed of particles being discharged through an orifice. The flow was characterized by definite regions within the bed where the particles had different velocities. This flow pattern has been used as a second explanation for the higher flow rates obtained with longer capillaries by Bingham and Wikoff.² The contention is that longer tubes favor the development of plug flow instead of turbulent flow. The plug flow will give higher efflux rates.

Brown⁵ has shown that a true plug flow, in which all particles of the moving bed have similar velocities, may be induced by merely fixing a few widely spaced horizontal rods at strategic points inside the vessel.

Oyama and Nagano⁶ studied the discharge rate of solid particles from an orifice steeped in water. Their results indicate also that the discharge rate is proportional to $D_o^{2.5}$ for sand, diatomaceous earth, and marble. They found a direct proportionality between discharge rate and particle diameter as long as the D_o/D_p was larger than 7. At values lower than 7, the particles would bridge the orifice and completely stop the flow. However, they found that the discharge rate was approximately proportional to $D_p^{0.5}$.

Mehring⁷ has reported that the discharge rate of the particles in an air atmosphere is inversely proportional to particle size. In this case the main factor which affects the discharge rate is simply the friction between the particles and between the particles and the wall.

In Oyama and Nagano's⁶ experiments, the liquid is completely enclosed, thus the same volume of water has to flow up the orifice as the volume of particles flowing down.

Kuwai⁸ studied the discharge of solid particles under low air pressures. His results indicate a direct proportionality between the particle flow rate and the driving force or air pressure. The particle flow rate was found to be inversely proportional to the particle diameter at a constant pressure for any one of the orifices tested. Also, the flow rate was affected by the orifice diameter, vessel diameter, and the bed height. Higher bed heights gave lower particle flow rates. The flow rates increased with increasing orifice diameters and also with increasing vessel diameter for any constant orifice size. However, the increase with vessel diameter gradually approached a constant value.

Experimental Work.—All of the experimental flow-rate data were taken, using solid particles made of the following three different materials.

1. Silicon dioxide: The silicon dioxide particles were obtained from the Ottawa Silica Sand Company of Ottawa, Illinois. The sand was not of an even particle size, and it had to be classified into "cuts" of different sizes by screening. Flow-rate data were obtained using "cuts" of 80/100 mesh, 140/200 mesh, and 200/325 mesh.

2. Copper: The copper shot was obtained from the Metals Disintegrating Company, Elizabeth, New Jersey. It also was not of a regular size and had to be classified. The flow-rate data were obtained, using the "cut" of 140/200 mesh.

3. Lead: The lead shot was also obtained from the Metals Disintegrating Company. Since it also was not of a regular size, it had to be classified by screening into "cuts" of different mesh sizes. The flow-rate data were obtained, using the "cut" of 140/200 mesh.

The orifice plates were made of brass, and they were 0.40 inch thick. The orifices were 0.10, 0.15, and 0.20 inch in diameter and 0.30 inch long. The greatest portion of the flow-rate data was taken, using the above orifices. However, a slight amount of work was done with sharp-edge orifices, having the same diameters as the straight ones.

All of the experimental flow-rate data of particles flowing downward through orifices were taken, using the continuous flow unit shown schematically in Fig. 24. Preliminary experiments in a batch system indicated the need for a

continuous system if reproducible data were to result. The unit consists of the following parts:

<u>Part No.</u>	<u>Name</u>
1	Particle reservoir
2	Orifice plate
3	Particle-receiving reservoir
4	Particle-water ejector
5	Water-recirculating pump
6	Pressure-control valve
7	Siphon-level control
8	Orifice-pressure tap
9	Water manometer to measure orifice pressure drop
10	Mercury manometer to measure over-all bed-pressure drop
11	Particle-dispersing baffle
12	Particle-water low-density line
13	Water-overflow line
14	Bucket
15	Ejector-water-control valve
16	Pump-recycle valve

The very first thing done in getting the unit ready for operation was to fill the bucket (14) with clear water. The ejector-water-control valve (15) was closed, and the pump-recycle valve (16) was opened all the way. The particle-receiving reservoir (3) was filled with clear water to the overflow level (13). The water-recirculating pump (5) was started, and the ejector-water-control valve (15) was opened all the way. The solid particles to be worked with were poured into the particle-receiving reservoir (3), and the pump-recycle valve (16) was closed slowly. As soon as the water started operating the ejector (4), the particles were conveyed to the particle reservoir (1) as a low-density slurry.

The pressure-control valve (6) was opened all the way, and a finger was held against the orifice (2) until all of the particles had been carried to the particle reservoir (1). The particle-receiving reservoir (3) was kept full of water at all times during the loading operation. The flow rate of the paste through the orifice was controlled by means of the pressure-control valve (6). Closing this valve increases the pressure inside the particle reservoir (1), thus increasing the flow rate of the particle paste through the orifice. A very fine control of the pressure was obtained by means of the siphon-level control (7) which is movable up or down.

The particle paste and the overflow water from the particle reservoir (1) are both received by the particle-receiving reservoir (3). The particles settle to the bottom, where they are picked up by the particle-water ejector (4) and are returned to the particle reservoir (1). The overflow of the particle-receiving reservoir (3) is returned (13) to the bucket (14), where it

is used by the pump (5) to operate the particle-water ejector (4).

The pressure drop across the orifice (2) is read from the water manometer (9), which is connected to the orifice-pressure tap (8). The overall bed-pressure drop is read from the mercury manometer (10), which is connected to the orifice-pressure tap (8) and the tap of the particle reservoir (1).

The continuous flow unit proved to be very satisfactory for taking the flow-rate data of a paste of particles flowing downward through an orifice.

The following procedure was used while taking the flow-rate data of the particle paste through the orifice.

The pressure-control valve (6) was set at a point, and the operator waited a sufficient length of time in order to obtain a steady state which was indicated by the constancy of the reading in the water manometer (9). Usually it would take from fifteen to thirty minutes to reach a steady state. The longer times were required when working with the smaller particles. This was due mainly to the plugging of the pressure tap with particles and the resulting slow response of the manometer.

The paste of particles was collected for a certain length of time in a tared calibrated glass cylinder. The collection time was recorded by a stop watch. Each run consisted of recording the following data: Reading of the water manometer (9), reading of the mercury manometer (10), collecting time as indicated by stop watch, total volume of paste (particles plus water) collected, and the gross weight of the calibrated glass cylinder.

The reading of the settled volume of sand in each run could not be used as a basis to determine the actual volume of sand, dry basis, flowing through the orifice. There was always the possibility that the sand would pack at different porosities when it settled in the calibrated cylinder. Thus, the actual volume of dry sand collected in each run was calculated in the following manner.

The total volume of the paste collected in each run has to be equal to the dry particle volume plus the volume of the water, thus

$$V_T = V_S + V_W \quad (1)$$

$$\therefore V_W = V_T - V_S \quad (2)$$

Also, the total weight of the paste collected in each run has to be equal to the weight of the dry sand collected plus the weight of the water, thus

$$W_T = W_S + W_W \quad (3)$$

or
$$W_T = V_S \rho_S + V_W \rho_W \quad (4)$$

Substituting Equation 2,

$$W_T = V_S \rho_S + (V_T - V_S) \rho_W \quad (5)$$

$$W_T = V_S (\rho_S - \rho_W) + V_T \rho_W \quad (6)$$

$$V_S = \frac{W_T - V_T \rho_W}{(\rho_S - \rho_W)} \quad (7)$$

The volume of solid particles, as obtained by using Equation 7, is the actual dry volume of the solid-particle material flowing through the orifice during any one of the runs. The volume fraction of water collected in each run was calculated by a material balance, using Equation 2.

All of the paste-flow-rate data through orifices, reported herein, are expressed in terms of cubic centimeters of the dry solid-particle material per minute.

Results and Correlation.—The experimentally determined data are shown in Figs. 25 through 29, which are plots of pressure drop across the orifice versus solids flow rate with orifice diameter as the parameter. Each figure is for a constant particle diameter and particle material (constant specific gravity).

Each one of the figures indicates a straight-line relationship between the flow rate and the pressure drop across the orifice. Thus, it seems possible to express the flow rate in terms of the pressure drop across the orifice as follows:

$$\Delta P = \eta W + C_1 \quad , \quad (8)$$

where η = slope of the straight line relating flow rate and pressure, drops for specific particles and orifice diameters and

C_1 = the intercept on the ΔP axis at zero flow rates.

Thus,

$$W = \frac{\Delta P - C_1}{\eta} \quad (9)$$

The data also indicate that η is dependent only on the orifice diameter at any constant particle size. Therefore, it indicates that η can be expressed as:

$$\eta = f_1(D_o) \quad (10)$$

or

$$\eta = f_2(D_o/D_p) \quad (11)$$

Both functions 10 and 11 were treated by means of graphical procedures. Equation 10 yielded a straight-line relationship when the logarithm of η was plotted versus the reciprocal of the orifice diameter. The particle diameter was used as the parameter, as shown in Fig. 30. Thus, the graph yields the following relationship between η and D_o :

$$\log \eta = a(1/D_o) + C_2, \quad (12)$$

where

a = slope of the straight lines relating $\log \eta$ versus $(1/D_o)$ and

C_2 = the intercept of the lines on the $(1/D_o)$ axis when $\eta = 1.0$.

The intercept value, C_2 , is different for each particle size studied, as of now. All of the experimental flow-rate data indicate that

$$C_2 = f_3(D_p) \quad (13)$$

Attempts to obtain a straight-line relationship from Equation 13 were not very fruitful. However, Fig. 31 shows the relationship between C_2 and the particle diameter, D_p . This figure brings up the fact that it is necessary to obtain more data, especially in the particle size range of 100/150 mesh. These screen-mesh numbers represent an average particle diameter of approximately 0.0049 inch. These data would definitely show whether there is a break in the C_2 versus D_p correlation at particle diameters of approximately 0.003 inch.

Using the data available at the present time one can assume that two straight-line functions represent the relationship between C_2 and the particle diameter. One of the functions represents the data including particle diameters from 140/200 to 200/325 mesh, and the other represents the data including particle diameters from 80/100 to 140/200 mesh.

Thus, we obtain the following relationships:

for particle diameters from 140/200 to 200/325 mesh,

$$C_2 = mD_p + C_4 \quad (14)$$

and for particle diameters from 80/100 to 140/200 mesh,

$$C_2 = bD_p + C_3, \quad (15)$$

where

m and b = slopes of the C_2 versus D_p plot and

C_4 and C_3 = corresponding intercepts when $C_2 = 0$.

The constant C_1 of Equation 8 originates from the original plot of flow rates versus pressure drop across the orifice. It can be seen that the value of C_1 obtained with the flow data of SiO_2 remains constant for any particle or orifice diameter tested. This fact indicates the possibility of correlating C_1 by Equation 15;

$$C_1 = f(\rho_p) \quad (16)$$

Further analysis of the intercept, C_1 , obtained with copper and lead, yielded Fig. 32. The point representing CaCO_3 was obtained from the data published by Kuwai.⁸ He used air instead of water as the driving medium, which makes the correlation more surprising since it would be expected that buoyancy would play an important part. No explanation can be given, at the present time, for this. Writing the equation for Fig. 32, we obtain:

$$C_1 = Q(1/\rho) + C_5, \quad (17)$$

where

Q = slope of the C_1 versus $1/\rho$ plot and

C_5 = intercept when $C_1 = 0$.

It is expected that the final relationship of the intercept C_1 and the specific gravity of the particle material will keep the general shape of Equation 17. However, the intercept, C_5 , might vary due to orifice-entrance effects, and the location of the orifice-pressure tap. These facts indicate the desirability of studying the orifice-entrance effects.

The final tentative correlation for the flow rate of a paste of particles flowing downward through an orifice is obtained as follows:

Substitute Equation 12 into Equation 9

$$W = \frac{\Delta P - C_1}{2.303 e^{a/D_0} + C_2} \quad (18)$$

Substitute now Equation 17 into Equation 18

$$W = \frac{\Delta P - Q/\rho_p - C_5}{2.303 e^{a/D_0} + C_2} \quad (19)$$

Since the C_2 values were expressed with two relationships, each one for a specific range of particle sizes, substituting Equations 14 and 15 into Equation 19, we obtain the final general correlation.

For particle diameter ranging from 140/200 to 200/235 mesh:

$$W = \frac{\Delta P - Q/\rho_p - C_5}{2.303 e^{a/D_0} + mD_p + C_4} \quad (20)$$

For particle diameters ranging from 80/100 to 140/200 mesh:

$$W = \frac{\Delta P - Q/\rho_p - C_5}{2.303 e^{a/D_0} + bD_p + C_3}$$

The values of the constants Q , a , b , m , C_3 , C_4 , and C_5 are given in Table II.

TABLE II

VALUE OF CONSTANTS FOR THE FINAL GENERAL CORRELATION

$$Q = 5.555$$

$$a = 0.01621$$

$$b = 0.09525$$

$$m = 1.3$$

$$C_3 = -1.002215$$

$$C_4 = -1.00581$$

$$C_5 = 0.59$$

COEFFICIENT OF FRICTION

Until recently the data on paste flow, even for upward flow, showed, what appeared to be a substantial frictional effect due, apparently, to the behavior of the moving mass of particles. In the light of these apparent facts, it was important to attempt to relate the frictional properties of the paste in nonflow systems with that in flow systems. The hope was that from measurements of "viscosity" or a coefficient of friction, taken with, perhaps, a concentric cylinder viscometer, one could predict the pressure-drop-flow-rate relationship for the same paste flowing in a tube.

Two techniques were investigated. The first consisted of simply pulling a loaded flat-plane sled across a layer of paste and finding the relationship between frictional and normal forces. This still left the problem of evaluating the normal forces in an actual paste-flow system. The second technique took in more of the complete stress system, and it involved the

measurement of the torque required to rotate a cylinder in a bed of the paste. The final form of the viscometer apparatus provided for the upward flow of water through the paste bed so that the condition in an upward flow tube could be simulated.

For several reasons, which will be brought up later, neither of these techniques has yielded results which are quantitatively reliable, but they are important in showing the high dependence of friction on bed density. Especially in the light of our present insight into paste flow, the frictional properties of the particle mass appear to be a passive reflection of the demands imposed by the conduit exit.

Sled Experiments.—The coefficients of friction between a glass plate and 150/200-mesh Ottawa sand paste, a zinc plate and 150/200-mesh Ottawa sand paste, and a zinc plate and -325-mesh iron-powder paste were determined with the sled apparatus. This apparatus consisted of a tank 30" long, 5" wide, and 3" high for holding the paste, a sled which could be loaded with weights, and an arrangement for pulling the sled by means of a wire, which passed over a pulley and was attached to a weight pan. With this apparatus one could measure normal force, the force required to start motion of the sled, and the force required to sustain motion.

The paste layer was prepared by spreading the mixture of solid particles and water over the tank bottom, tapping the tank for various lengths of time to increase bed density and finally by scraping the surface level. The bed density was determined from samples of the paste taken after each run.

The data are summarized in Figs. 33, 34, and 35, which are plots of coefficient of friction and volume-fraction solids in the paste. It can be seen that for the sand paste the coefficient drops abruptly as the bed density decreases below about 58% solids.

Viscometer Experiments.—Our early attempts to measure the "viscosity" of sedimented pastes by means of a "Brookfield" viscometer have been described in an earlier report. It turned out to be impossible to get any meaningful results by running the rotating cylinder in a beaker of paste due to the random variation of normal force on the cylinder. The use of this instrument was taken up again in conjunction with an arrangement for forcing water up through the paste bed.

As the water rate is increased, the point may be reached where the frictional pressure drop is equal to the head due to the buoyant weight of the solids. At this point the solid particles are, on the average, "weightless," and there should be no variation in normal force acting along the length of the cylinder. Further increase in water rate will result in an expansion of the bed and will still provide the characteristic of weightless particles. It might be mentioned that this is the only way, we can see, in which this instrument can be applied to dense paste systems with clear-cut significance.

A sketch of the apparatus is shown in Fig. 36. The volume of the container above the fritted disc was calibrated as a function of height so that the bed density for a known weight of solids could be determined from a measurement of the paste bed height. Three spindles were employed; all were 2" long from the bottom to the gauge mark, and they differed in diameters, which were 1/2", 3/4", and 1". The viscometer speeds were 1, 2, 5, and 10 rpm. Each unit on the torque dial is equal to 0.1025 gm cm.

The data obtained for 100/140-mesh Ottawa sand are presented in Fig. 37, a plot of torque dial reading versus fraction solids in the bed. Due to the "stick-slip" phenomenon, which is intensified by the torque-spring coupling in the drive shaft, the readings fluctuate widely and are shown as bars rather than points. There was a negligible effect of rotational speed in this and all other data which were taken on this system. The maximum scale reading is 500, and this controlled the highest bed density which could be run in the apparatus. Where data halts at a scale reading below 500, it indicates that any further increase in density (decrease in water rate) would cause the torque gauge to go off scale.

Data for 100/140-mesh copper shot and 100/120-mesh glass beads are shown in Figs. 38 and 39. All of these data are subject to uncertainty due both to the stick-slip effect and to the channeling which occurred at high water-flow rates.

Discussion of Results.—Coefficient of friction data, as determined by the sled method, would be useful if we had a way of evaluating the normal force acting in a paste-flow system. Since we do not, except for Delaplaine's data, no predictions based on these values are to be made at present. They are of present interest in showing that there is a significant relationship between coefficient of friction and volume-fraction solids.

The frictional effect in an upward flow system can be estimated from the viscometer data. Although the data are not extensive and reliable enough to support the argument rigorously, we can observe that shear stress (force per unit area of cylinder surface) is approximately constant with the cylinder diameter at the lower bed densities, i.e., torque is proportional to the square of the cylinder diameter. Assuming that this will hold for paste flow through tubes, we can estimate the frictional force exerted against the tube wall.

By extrapolation, we estimate the torque reading for the 1/2" diameter spindle in 100/140-mesh sand at 55% solids to be 1.5. Thus, the torque is 0.154 gm cm, and the shear stress is 0.0116 gm cm, and the shear stress is 0.0116 gm/cm². The ratio between frictional force and force due to the buoyant weight of the solids [at $(1-X) = .55$ for sand] is then computed to be $(0.051/D)$, where "D" is tube diameter in centimeters. For upward flow in a 1-cm diameter tube this indicates a frictional force equal to about 5% of the pressure drop at an overweight ratio of 1.0. In the same manner, we can

estimate that for a reading of 40 for copper shot at 55% solids the ratio of friction to bed-weight "head" would be $(0.14/D)$.

What with the uncertainties in the experimental measurement and the necessity for extrapolation to the loosely settled density of 0.55, this is not bad confirmation of the experimental observation that frictional effects are negligible for upward flow with a flushed exit. A closer check could be made by using more elaborate techniques and a viscometer fitted with a zero-displacement torque pickup. However, this is not warranted as a part of the study of paste flow since this technique is only valid for the upward flow case and direct experimental observation of pressure drop is simpler to accomplish.

EXPLORATORY EXPERIMENTS ON DOWNWARD AND HORIZONTAL FLOW SYSTEMS

One of the by-products of the recognition of the effect of the exit on upward flow was the realization that the exit could be equally important for downward and horizontal flow. Our previous experience had been that stratification occurred in these systems. Upon rerunning them, we found that uniformly dense flow could be attained in both systems if a restriction were placed at the tube exit.

It should be made clear that the downward flow system we refer to here is that case in which a downward leg is added to a hairpin system. Thus, the paste flows downward out of the reservoir, then upward, and finally downward again. In this case the ratio of liquid to solid is set by the upward flow leg, and, if the tube exit is unrestricted, this ratio is too high for the tube to run full. The solids will drop to the tube exit as individual particles, unless the flow rate is extremely high.

By putting a restriction at the tube exit, we in effect, impede the flow of particles more than the flow of liquid. The ratio of liquid to solid is set by the orifice diameter, as we see from the work on flow through orifices. Thus, eventually we should be able to predict the optimum size orifice just to keep the downward flow tube running full. To do so, we need know the characteristics of both the downward tube and the orifice.

Horizontal flow is subject to the same general reasoning as given for downward flow. If we could characterize the behavior of flow in a horizontal tube as well as in the exit orifice, we could design this type of system. Work along these lines is being planned for the near future.

Friction for horizontal flow will probably be high as compared to vertical flow. We can estimate the friction as follows.

For a differential cylindrical element of radius r and length dL , with its axis horizontal the force balance is described by:

$$0 = dF + \frac{\Delta P}{L} \pi r^2 dL - C_1 \rho_b \pi r^2 dL - \frac{2C_2 F}{r} dL \quad (15)$$

and by rearrangement

$$dF = \left[\frac{2C_2 F}{r} - \left(\frac{\Delta P}{L} - C_1 \rho_b \right) \pi r^2 \right] dL \quad (16)$$

where

C_1 = coefficient of friction, assume = 0.6 and

Other symbols are as described previously.

By integration of Equation 16 and substitution of numerical values for C_1 and C_2 , we get:

$$0.6 \left(\frac{L}{r} \right) = \ln \frac{\left[\frac{0.6F}{r} - \left(\frac{\Delta P}{L} - 0.6 \rho_b \right) \pi r^2 \right]}{\left[\frac{0.6F_0}{r} - \left(\frac{\Delta P}{L} - 0.6 \rho_b \right) \pi r^2 \right]} \quad (17)$$

By the same reasoning as was applied to Equation 9, we find that

$$\frac{0.6F_0}{r} \approx \left(\frac{\Delta P}{L} - 0.6 \rho_b \right) \pi r^2 \quad (18)$$

If F_0 , the force exerted against the exit orifice, were zero,

$$\frac{\Delta P}{L} = 0.6 \rho_b \quad (19)$$

This corresponds to an overweight ratio of 0.6. Since some force will be exerted against the orifice exit, the actual pressure drop will be higher than this. Probably an overweight ratio of 1.0 would be a fair approximation.

COMPLETE REACTOR FLOW SYSTEMS

The ultimate point of interest in this project is the utilization of a paste fuel in a nuclear-reactor system. The general requirements of such a system are as follows:

1. Paste flow passages must be small enough so that the required rate of heat transfer can be attained without necessitating a paste temperature approaching the sintering point.

2. Flow through all of the paste passages should be at a uniform rate and density.

3. The system should be "fail safe."

There are also the general ideals one would strive to attain, such as simplicity, low pressure drop, and ease of filling and emptying.

It is still our belief, as expressed in the previous report, that the high-density downward flow with low-density lift system offers greater promise than the hairpin type of system. For this reason the design concepts we have envisioned were all based on the low-density lift system. In any case, the major problem remains essentially the same, i.e., how to distribute the paste to the tops of the individual channels and collect it from the bottoms.

After having sketched a number of alternate designs, we found that practically all of our ideas for collection and distribution systems could be represented by two types. One type is illustrated in Fig. 40a and involves picking up the particles in a stream of sweep liquid, lifting the low-density slurry to the top of the reactor by means of an ejector pump, and then distributing the slurry over the tops of the paste channels so that the particles would settle out. This system would require additional fittings to permit withdrawal of the slurry from the reactor. The other type is shown in Fig. 41, and it involves the introduction of high-density paste from a separator outside the reactor, the movement of the paste at high-density from passage-outlet orifices to the ejector, and then low-density lift to the separator.

One can make variations on these basic types by providing conical top and bottom geometry to promote the movement of particles by gravity, or it might be desirable to vary the width of the distribution and collection channels along the radius of the cylinder, in order to attain optimum flow distribution and minimum holdup. Another possibility would be the provision of distribution and collection passages in the form of a spiral, which might offer less short-circuiting and fewer dead spots.

What it all boils down to is that we need to know more about flow through horizontal and inclined channels. This includes stratified, non-stratified, and low-density flow and there would be particular emphasis on radial flow with multiple inlets and outlets. Flow through orifices and the ejector-life system are also significant elements of design information, which are required.

The small (8" diameter) model, illustrated in Fig. 40b, was built to represent the flow system shown in Fig. 40a. A few runs were made with this model, but they were inconclusive, first because the holes in the perforated plate were too large and second because there were too many interdependent factors, each of which must be closely designed to match the others. This apparatus does have the very desirable feature of representing the paste passages by a perforated plate, and this will enable the investigation of full-scale distribution and pickup systems with relatively simple and inexpensive equipment.

It is planned that the investigation of complete reactor flow systems will form the major part of the program for next year. While the general form of the necessary investigation is shown in the above discussion, there are bound to be special problems appearing as new design concepts come to mind. Work will start on what looks like the most promising scheme—the outside-separator design, shown in Fig. 41.

REFERENCES

1. Leva, M., et al., "Fluid Flow Through Packed and Fluidized Systems," Bull. 504, U.S. Bureau of Mines (1951).
2. Bingham, E. C. and R. W. Wikoff, J. Rheol., 2, 395, 414, 416 (1931).
3. Wieghardt, K., Ingenieur-Archiv., 20, 109 (1952).
4. Brown, R. L. and P. G. W. Hawksley, Fuel, 26, 159 (1947).
5. Brown, R. L., Fuel, 29, 418 (1950).
6. Oyama, Y. and K. Nagano, Reports. Sci. Research Inst. (Japan), 29, 349-352 (1953).
7. Mehring, A. L., Ind. Eng. Chem., Anal. Ed., 3, 34 (1931).
8. Kuwai, G., Chem. Eng. Japan, 17, 453-9 (1953).

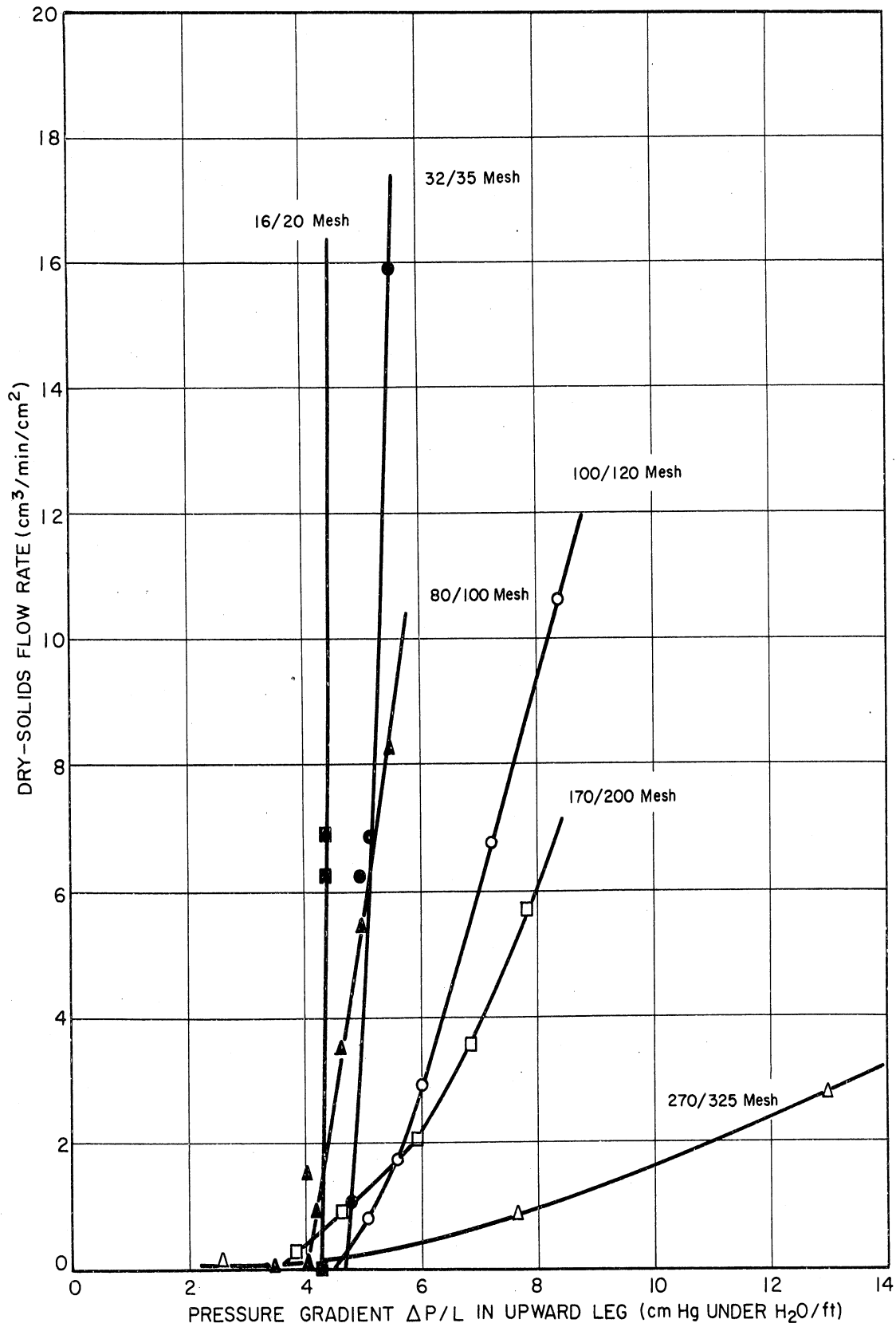


Fig. 2. Solids flow rate versus pressure drop for upward flow of glass beads in a 10.3-mm-ID hairpin with overflow exit.

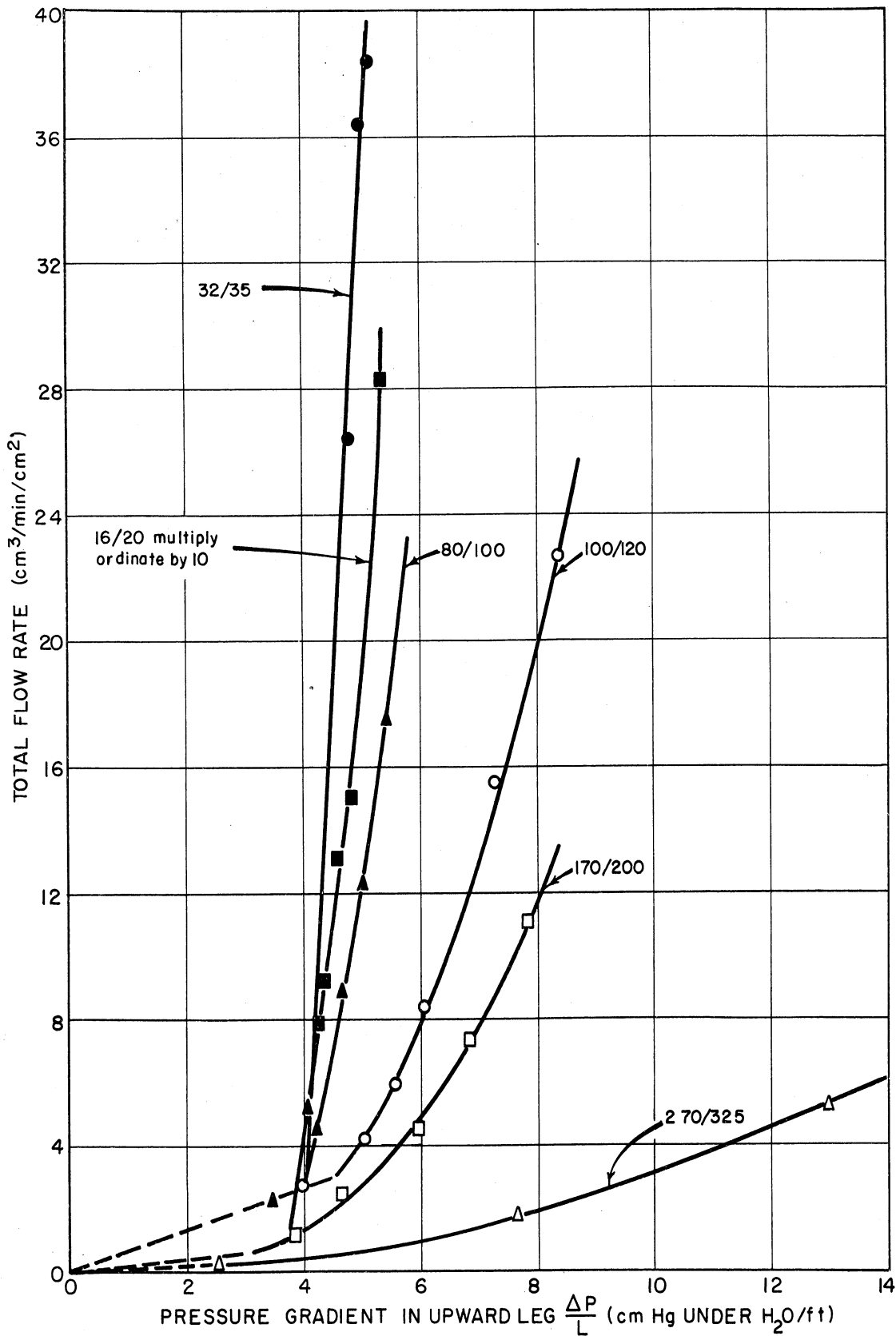


Fig. 3. Total flow rate versus pressure drop for upward flow of glass beads in a 10.3-mm-ID, 2-ft-long hairpin with overflow exit.

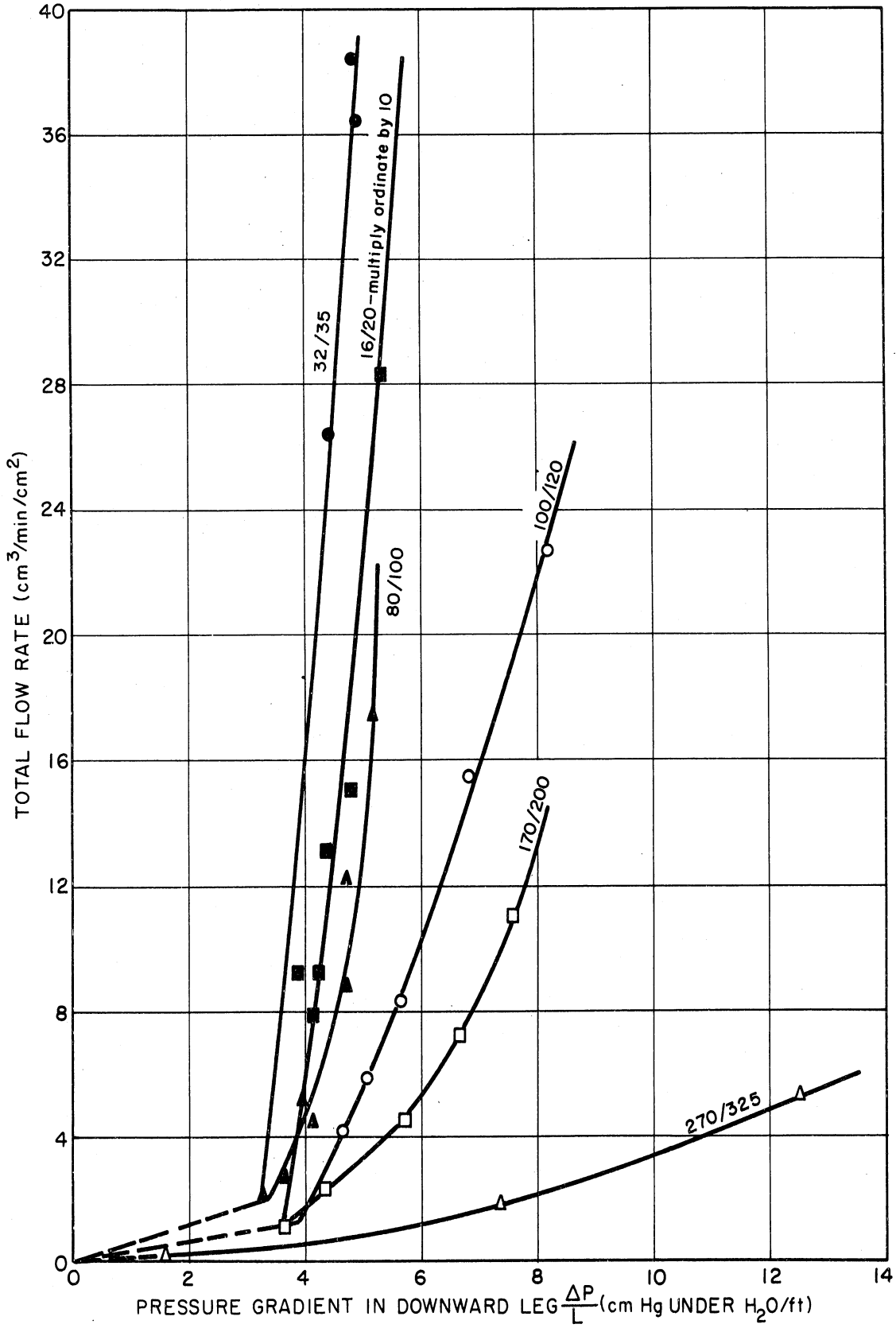


Fig. 4. Total flow rate versus pressure gradient for the downward flow of glass beads in a 10.3-mm-ID hairpin with overflow exit.

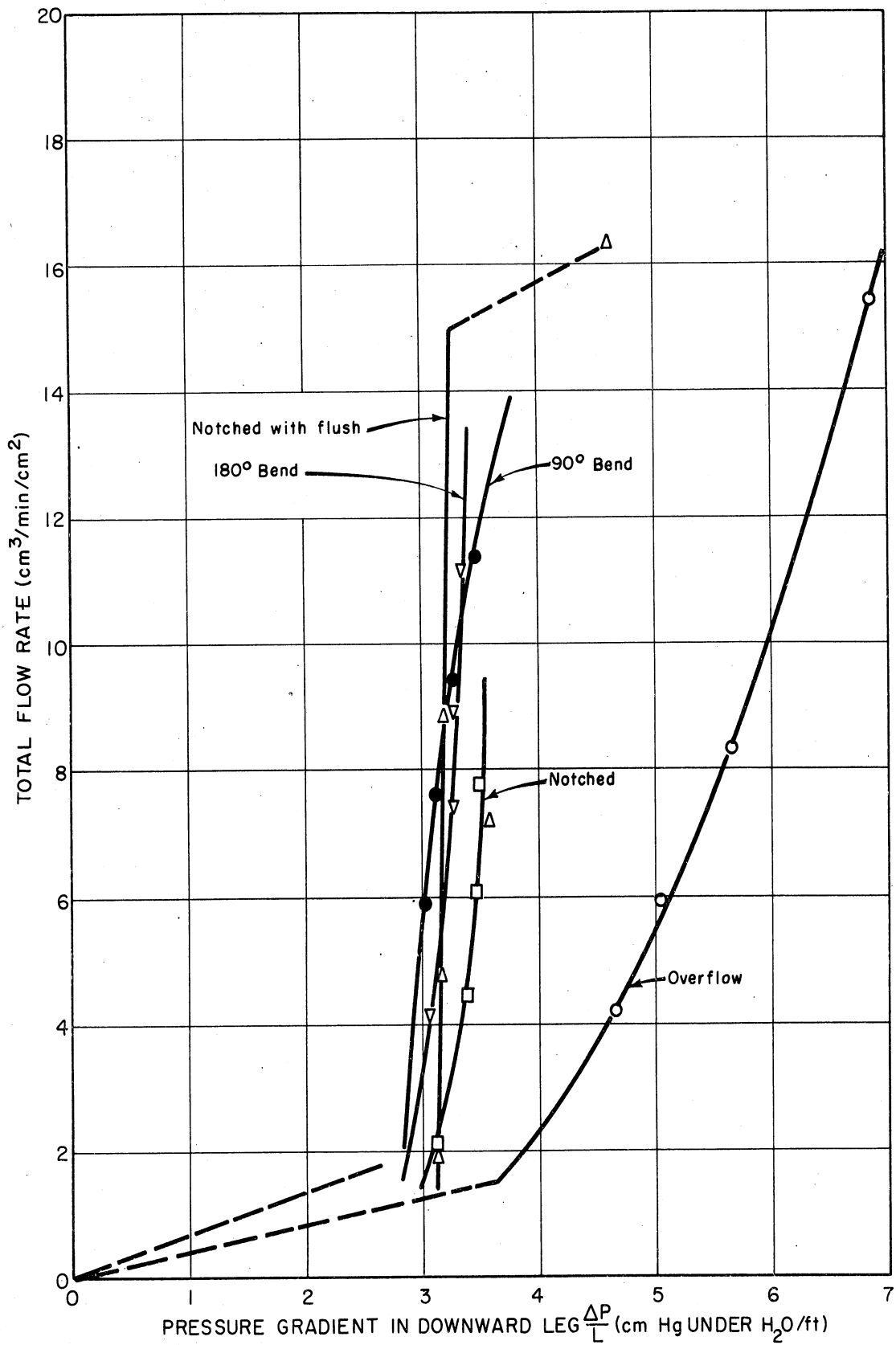


Fig. 5. Total flow rate versus pressure drop for downward flow of glass beads in a 10.3-mm-ID hairpin with various exit types.

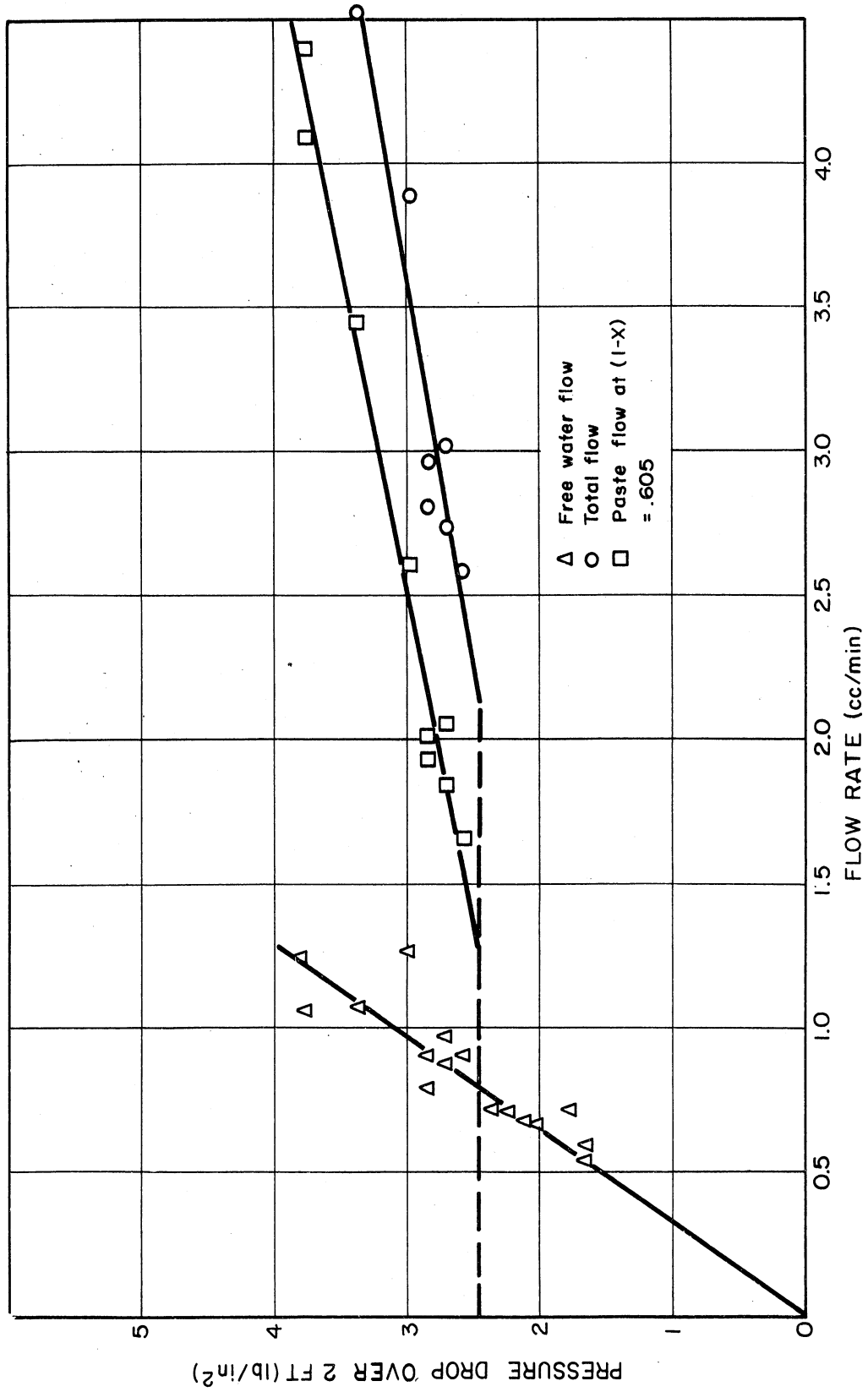


Fig. 6. Pressure drop versus flow rate for downward flow of 82-micron Ottawa sand in a 10.2-mm-ID, 2-ft-long hairpin with overflow exit.

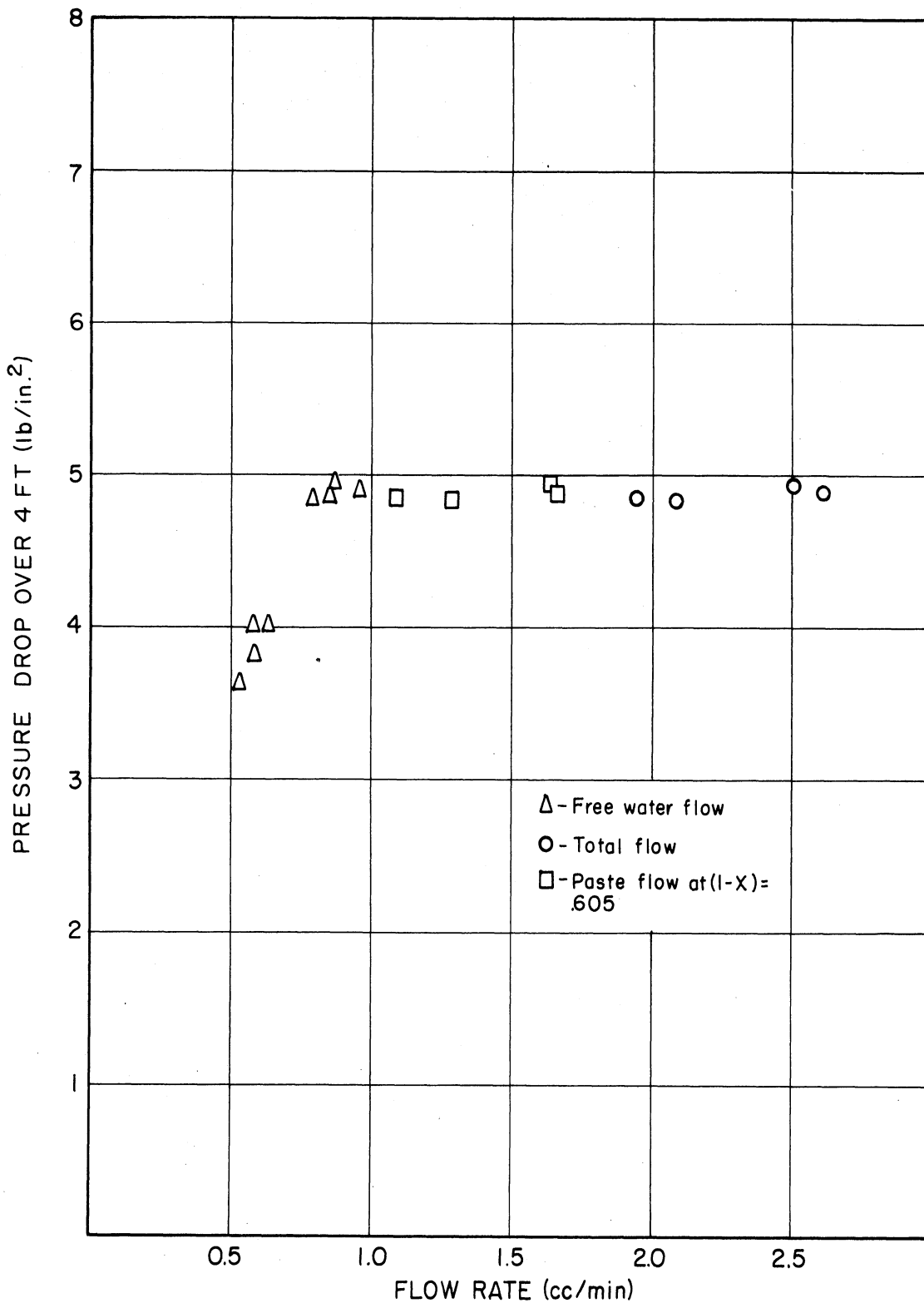


Fig. 7. Pressure drop versus flow rate for downward flow of 82-micron Ottawa sand in a 10.2-mm-ID, 4-ft-long hair-pin with overflow exit.

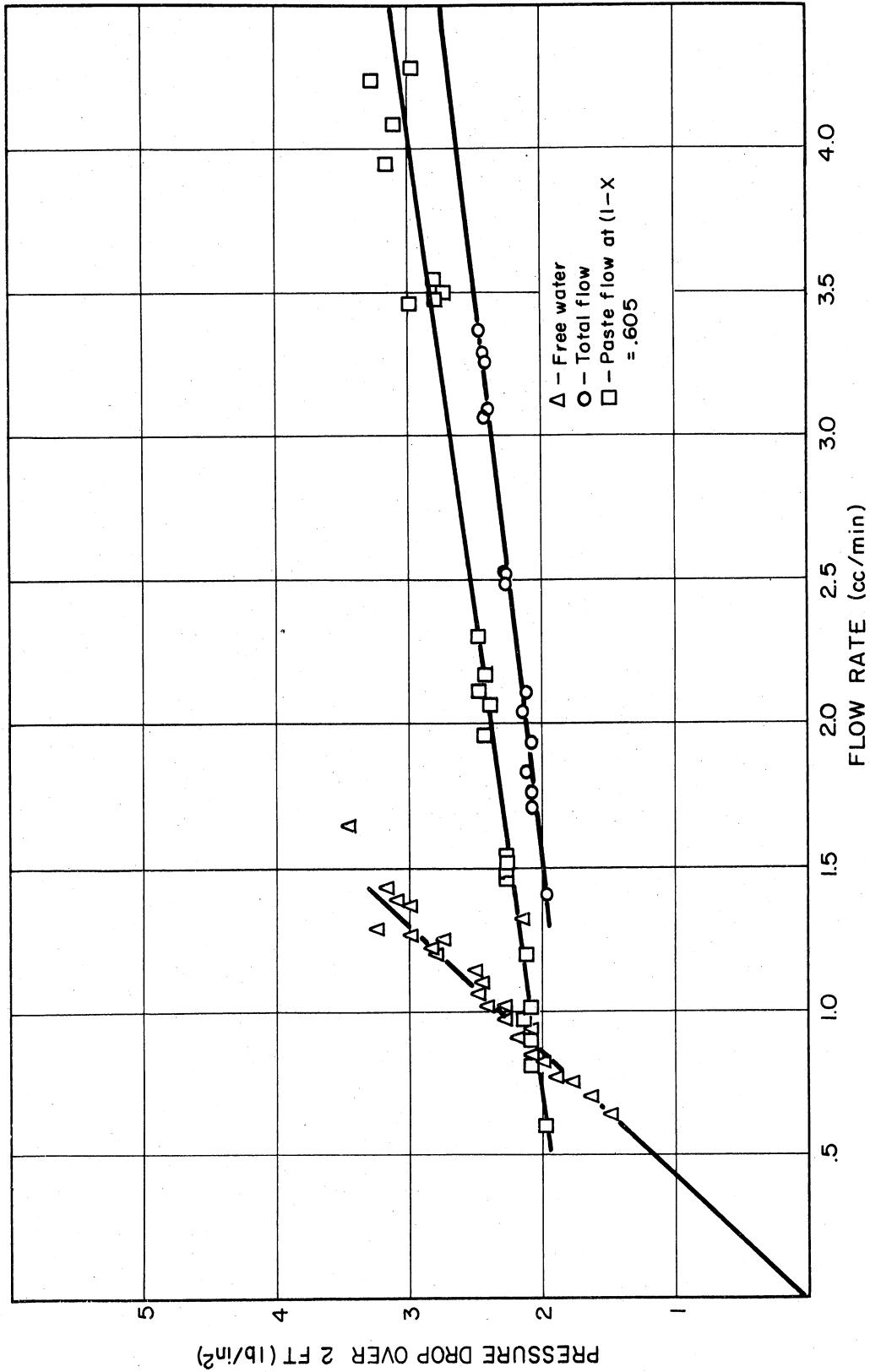


Fig. 8. Pressure drop versus flow rate for downward flow of 98-micron Ottawa sand in a 10.2-mm-ID, 2-ft-long hairpin with overflow exit.

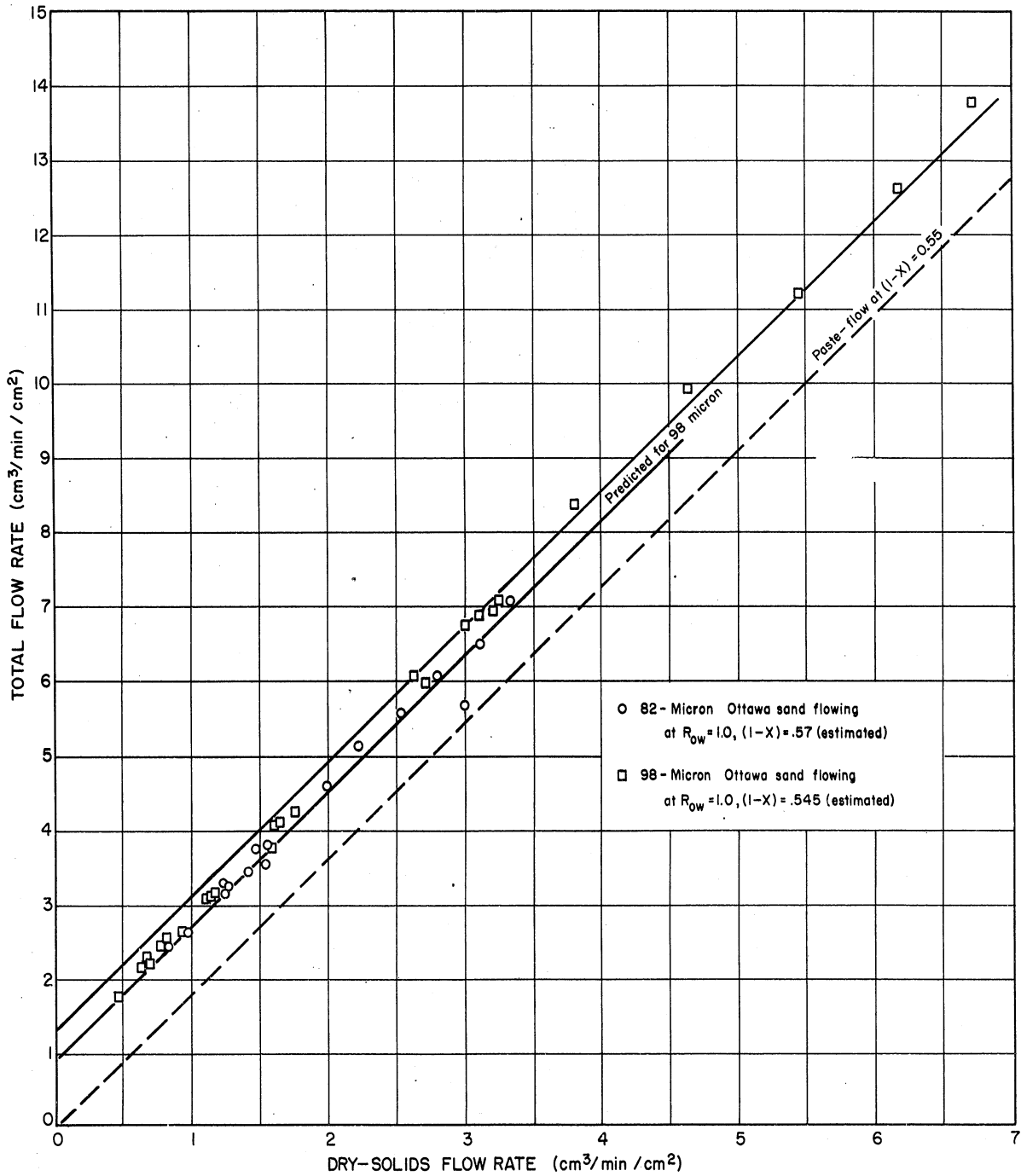


Fig. 9. Total flow rate versus solid flow rate for upward flow of Ottawa sand in a 10.2-mm-ID hairpin with overflow exit.

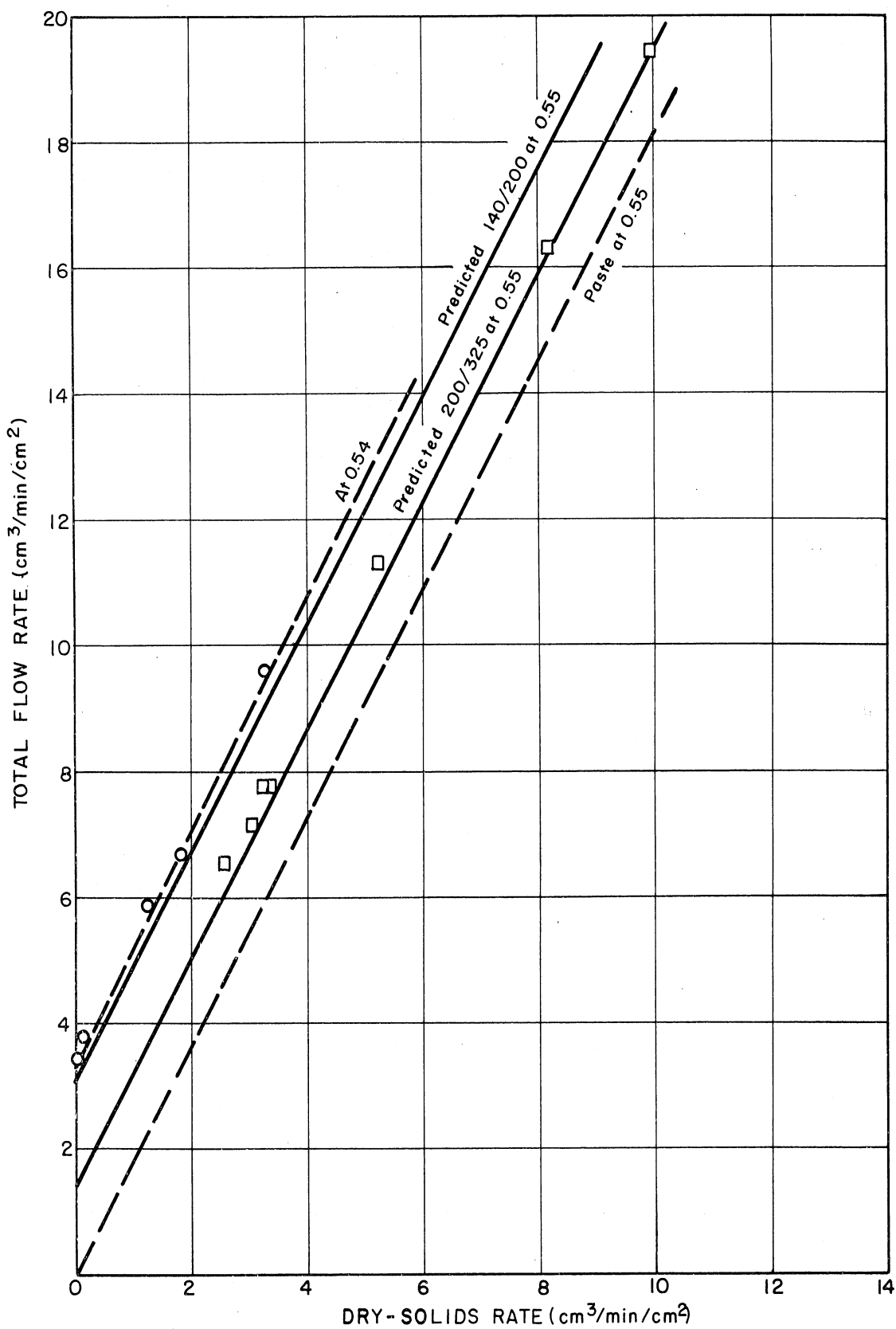


Fig. 10. Total flow rate versus solid flow rate for upward flow of copper shot in a 10.3-mm-ID hairpin with overflow exit.

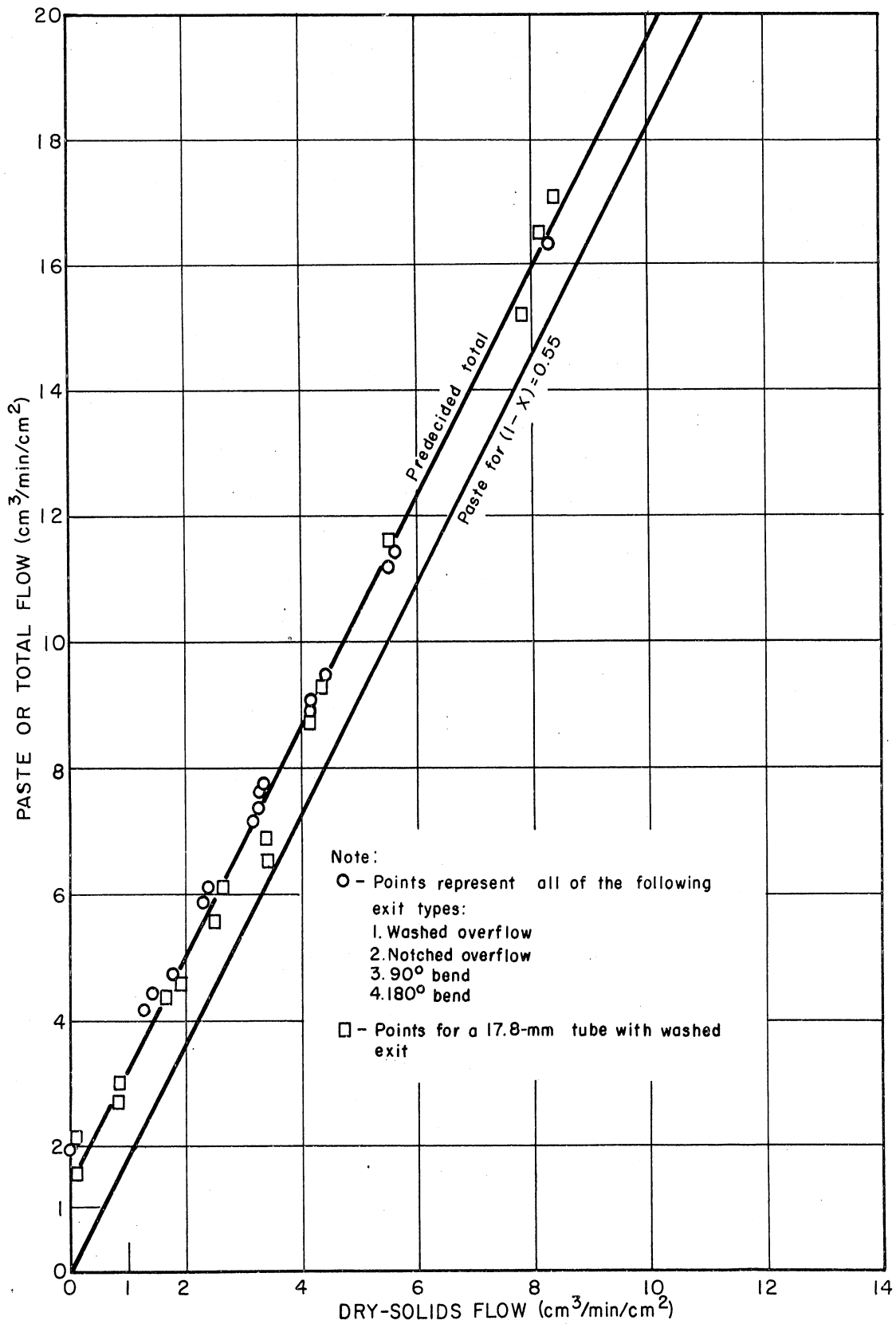


Fig. 11. Total flow rate versus solid flow rate for upward flow of 100/120-mesh glass beads in a 10.3-mm-ID tube with various exit types.

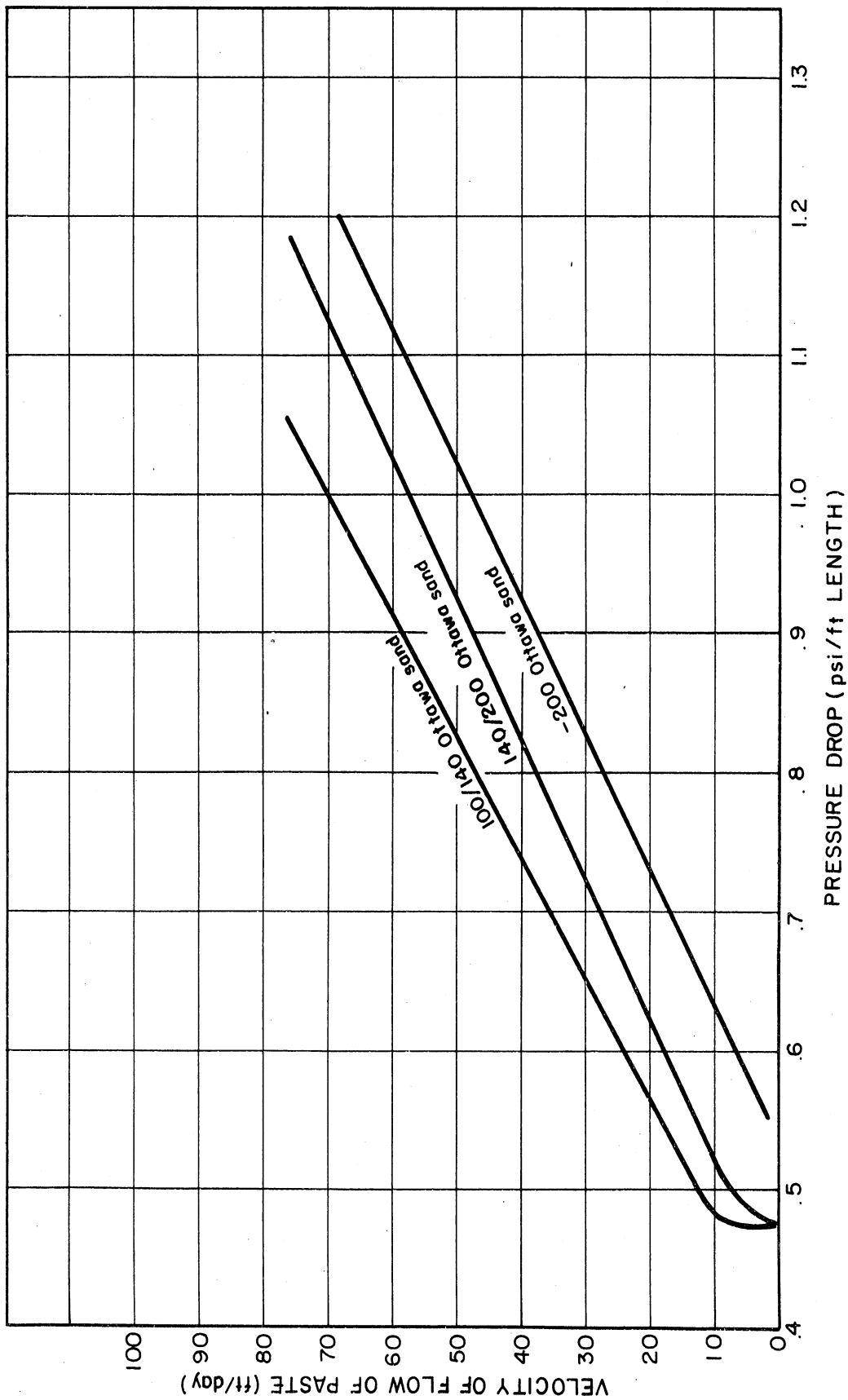


Fig. 12. Paste velocity versus pressure drop for downward flow of Ottawa sand in a 17.8-mm-ID, 4-ft-long hairpin with overflow exit.

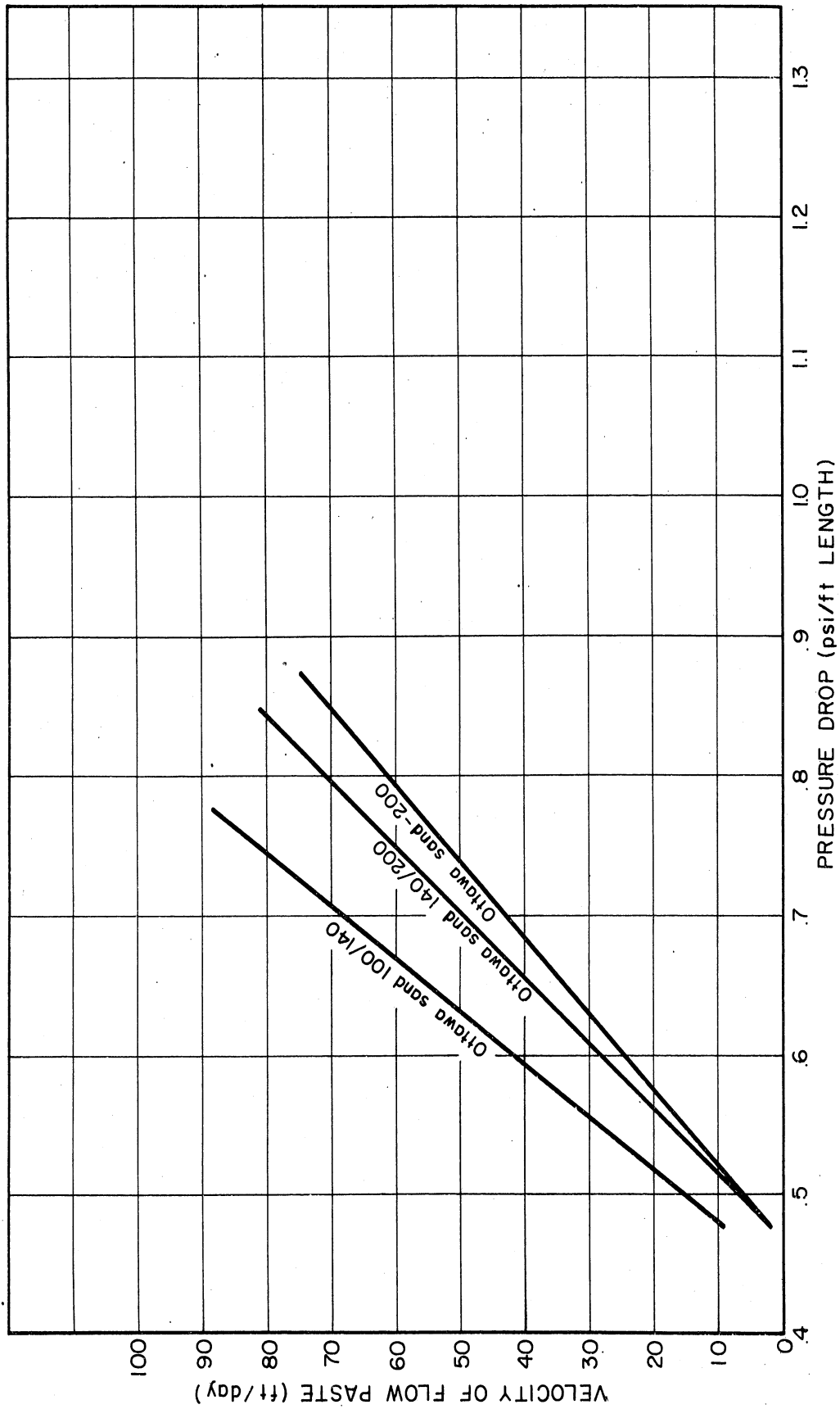


Fig. 13. Paste velocity versus pressure drop for upward flow of Ottawa sand in a 17.8-mm-ID, 4-ft-long hairpin with overflow exit.

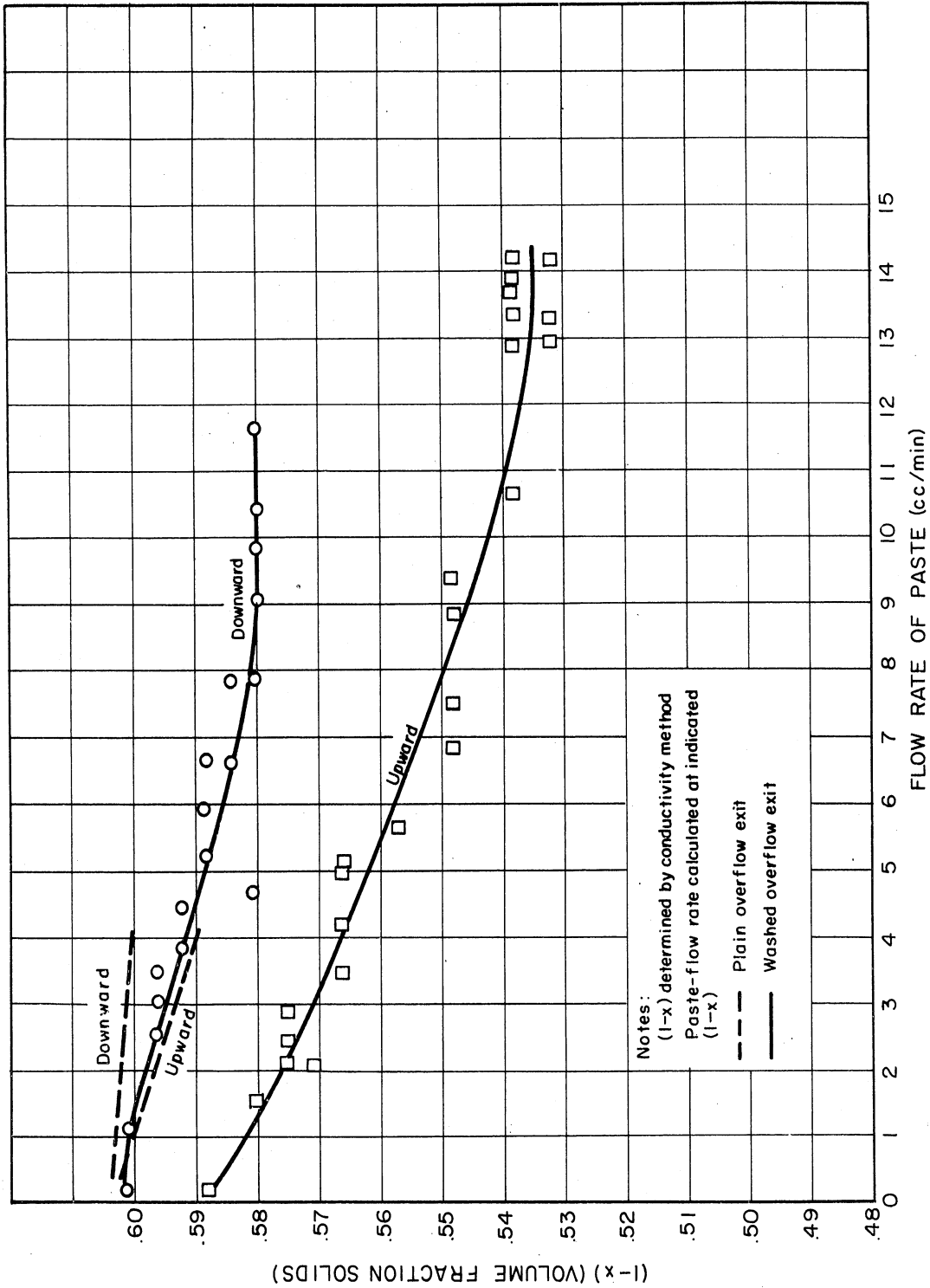


Fig. 14. Volume fraction solids versus paste flow rate for 100/140-mesh Ottawa sand in a 17.8-mm-ID hairpin and washed-overflow exits.

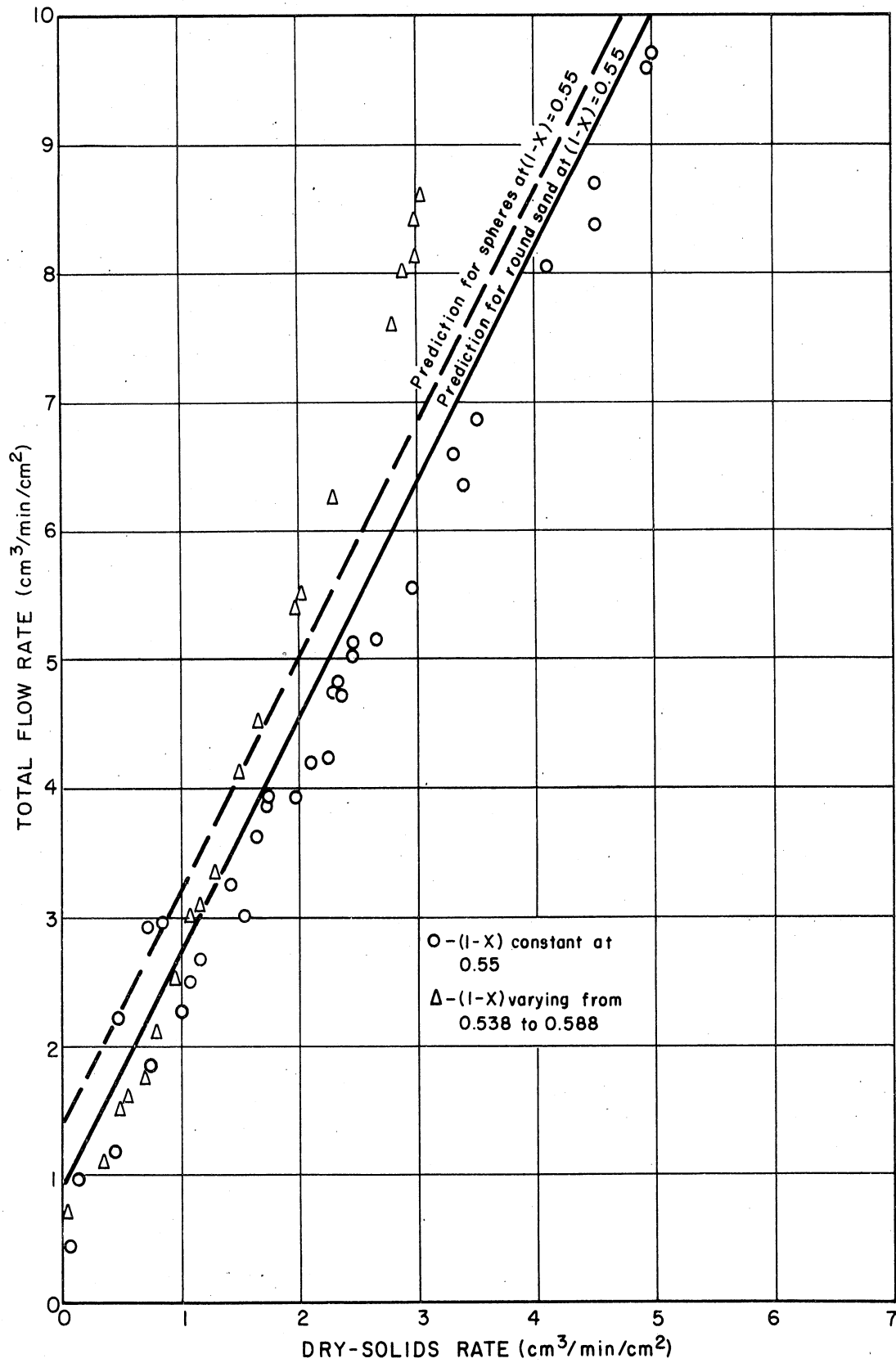


Fig. 15. Total flow rate versus solids flow rate for upward flow of 100/140-mesh Ottawa sand in a 17.8-mm-ID hairpin with washed exit.

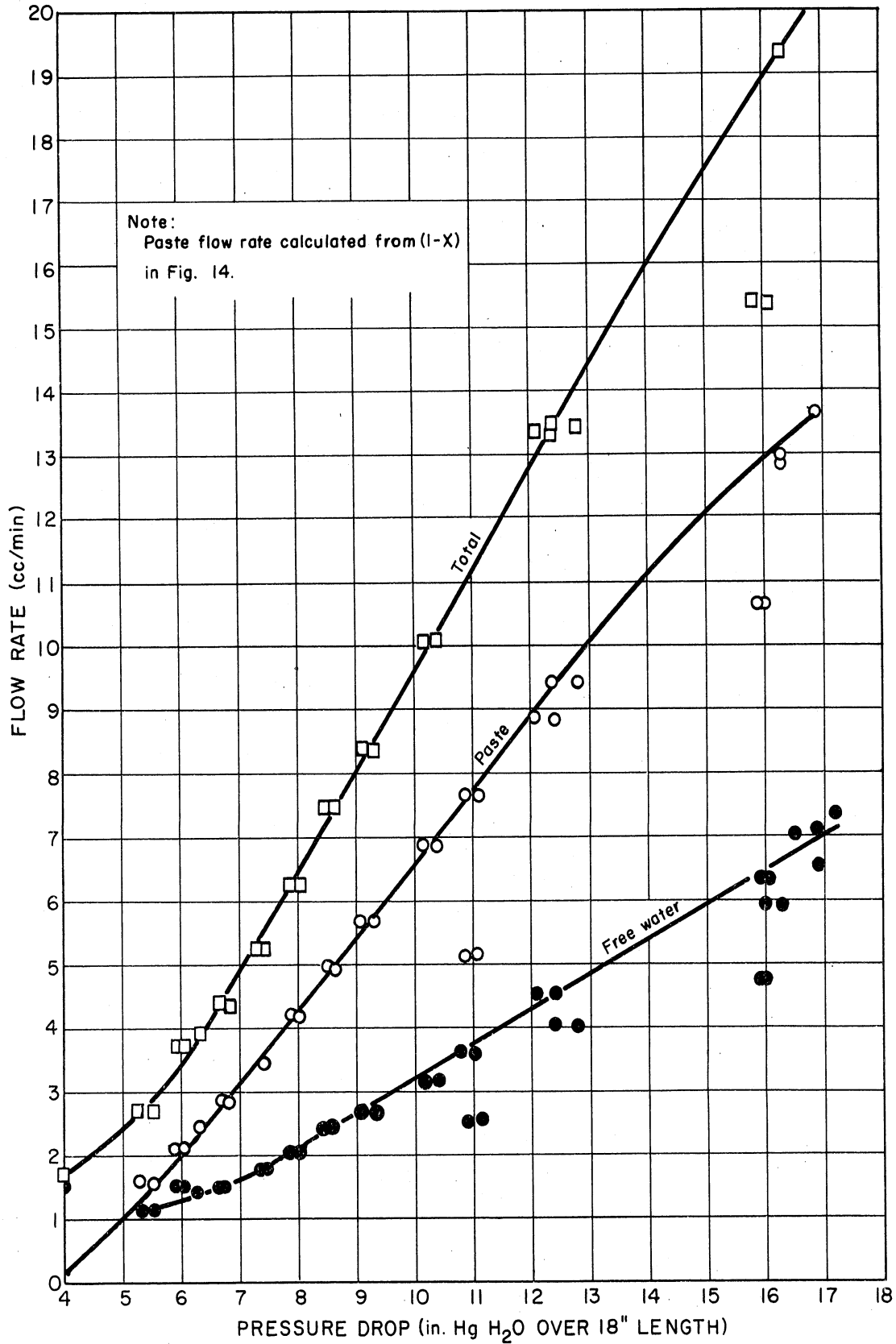


Fig. 16. Flow rates versus pressure drop for downward flow of 100/140-mesh Ottawa sand in a 17.8-mm-ID hairpin with washed exit.

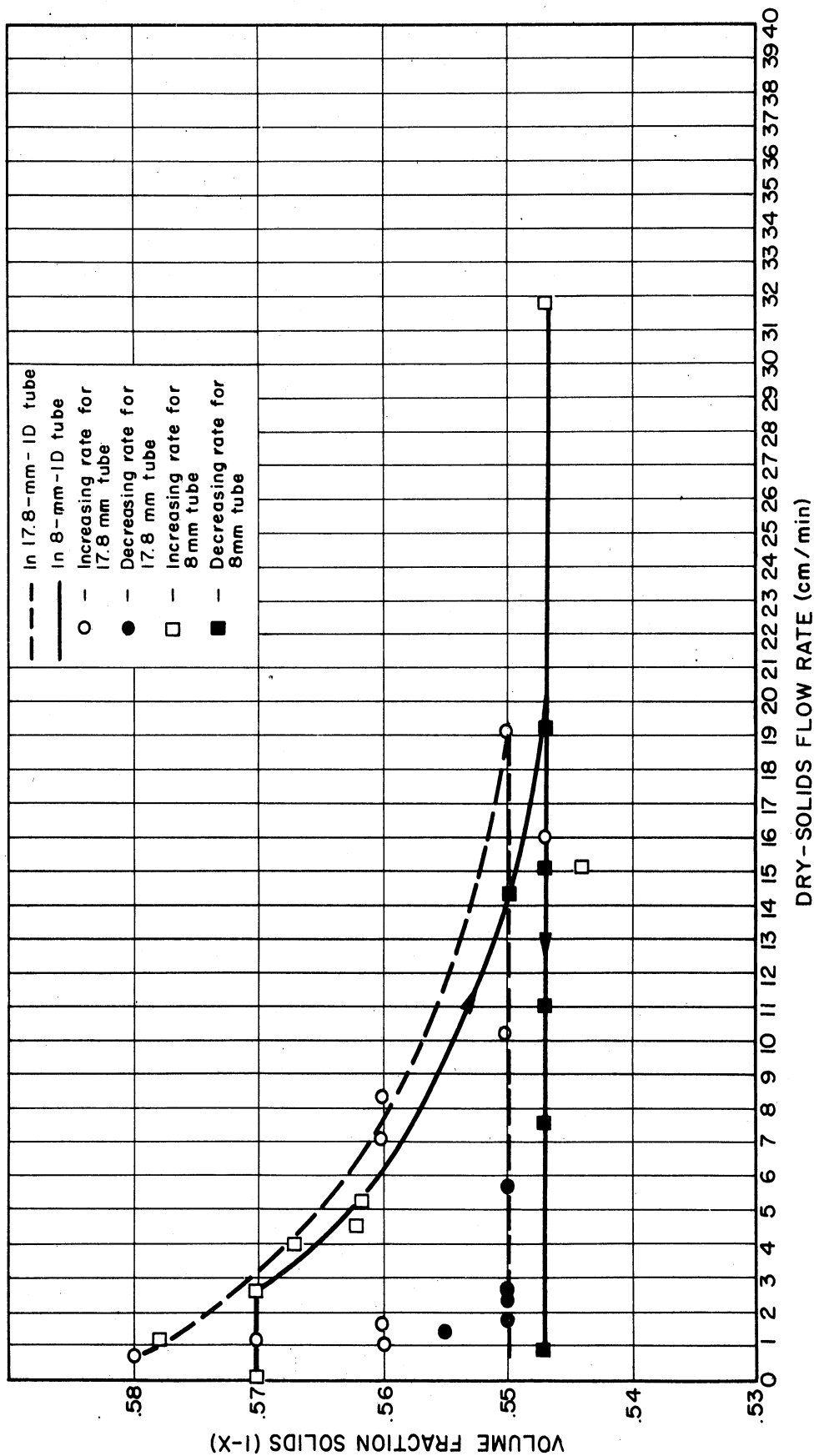


Fig. 17. Volume fraction solids versus solids flow rate for upward flow of 100/140-mesh Ottawa sand in 8-mm-ID and 17.8-mm-ID tubes. Porosity determined by electrical conductivity method.

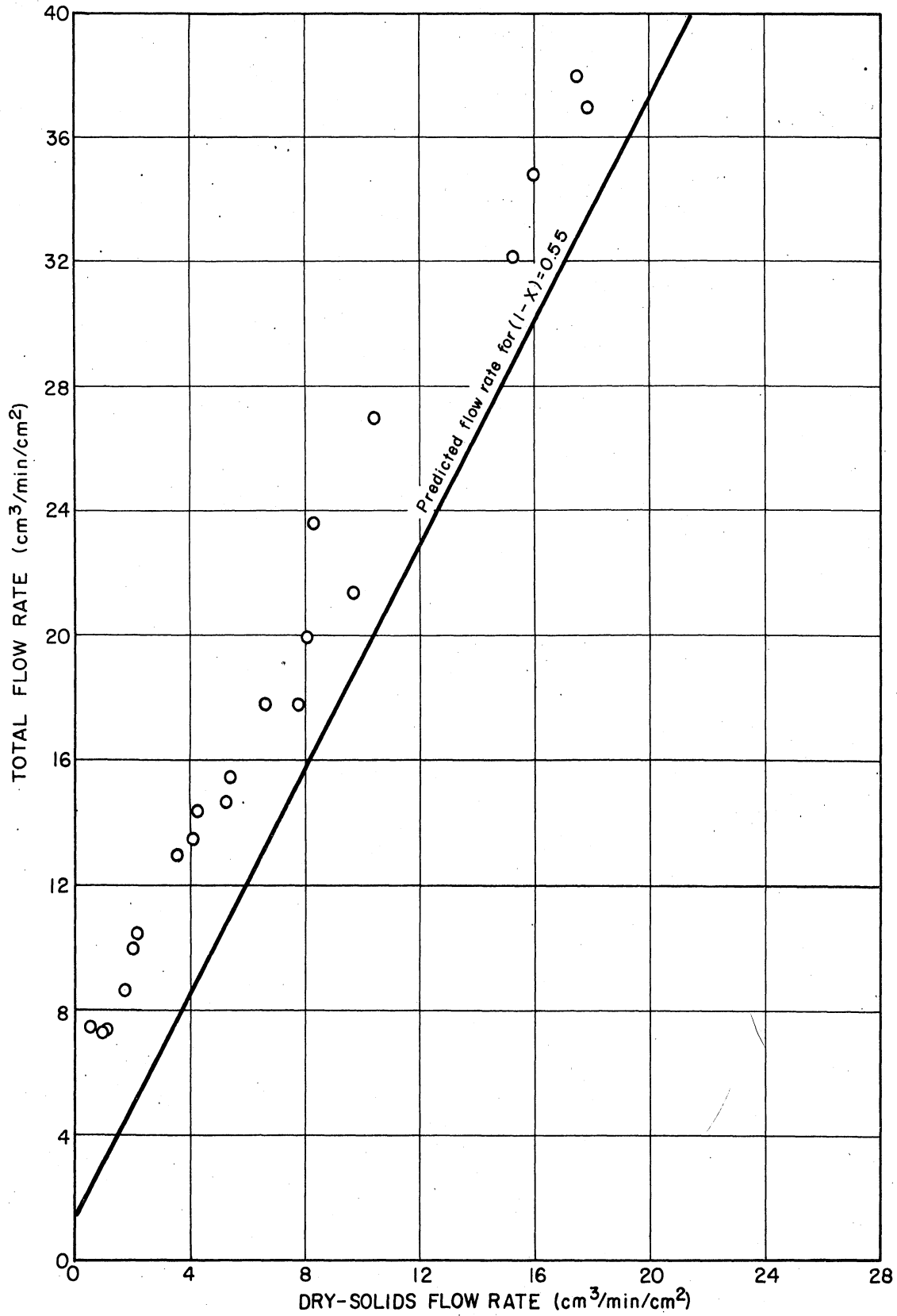


Fig. 18. Total flow rate versus solids flow rate for upward flow of 100/120-mesh glass beads in an 8-mm-ID hairpin with washed exit.

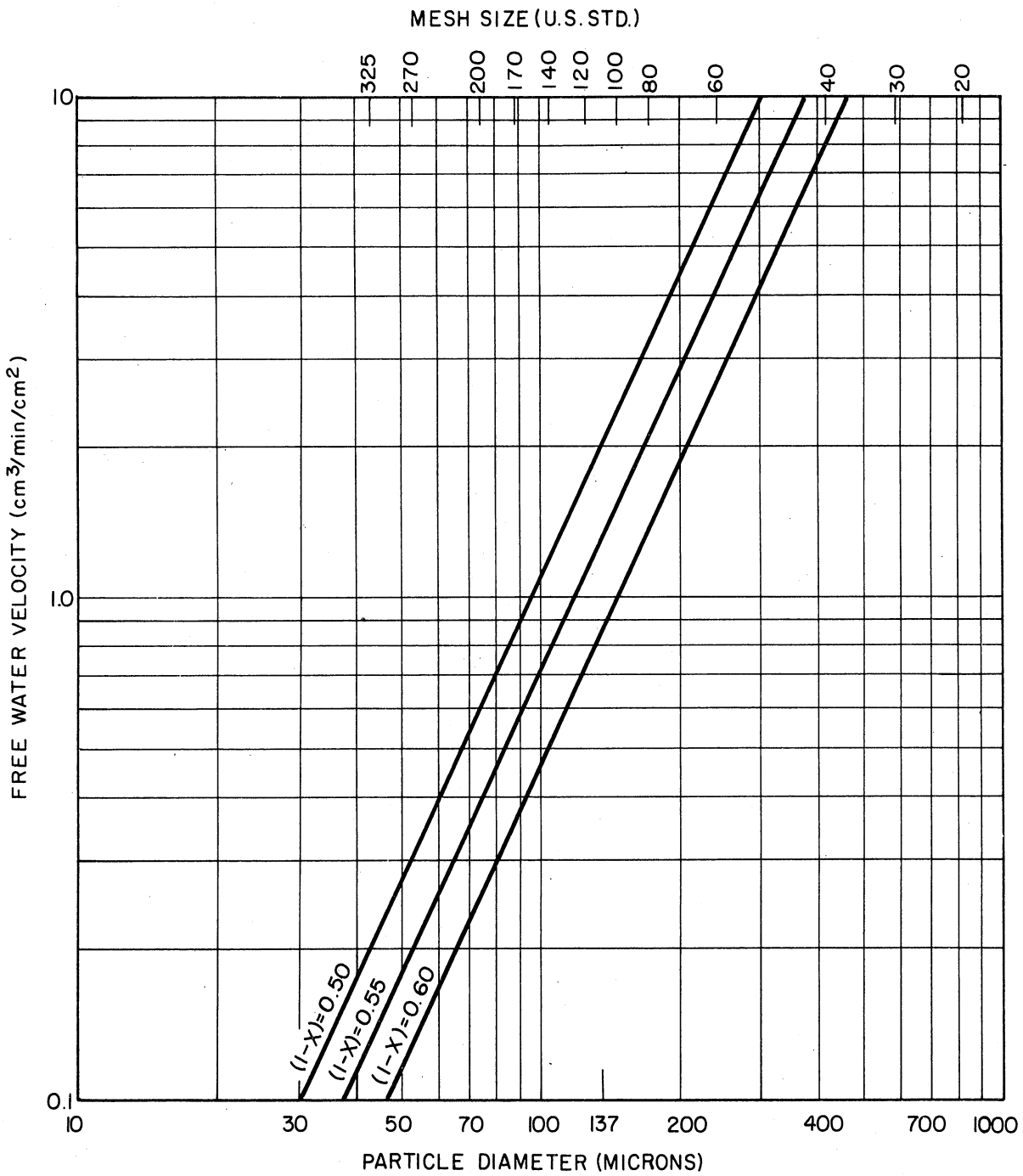


Fig. 19. Predicted free water velocity versus particle diameter with volume fraction solids as parameter for spheres with density of 2.49 gm/cm³ flowing upward at $R_{OW} = 1$.

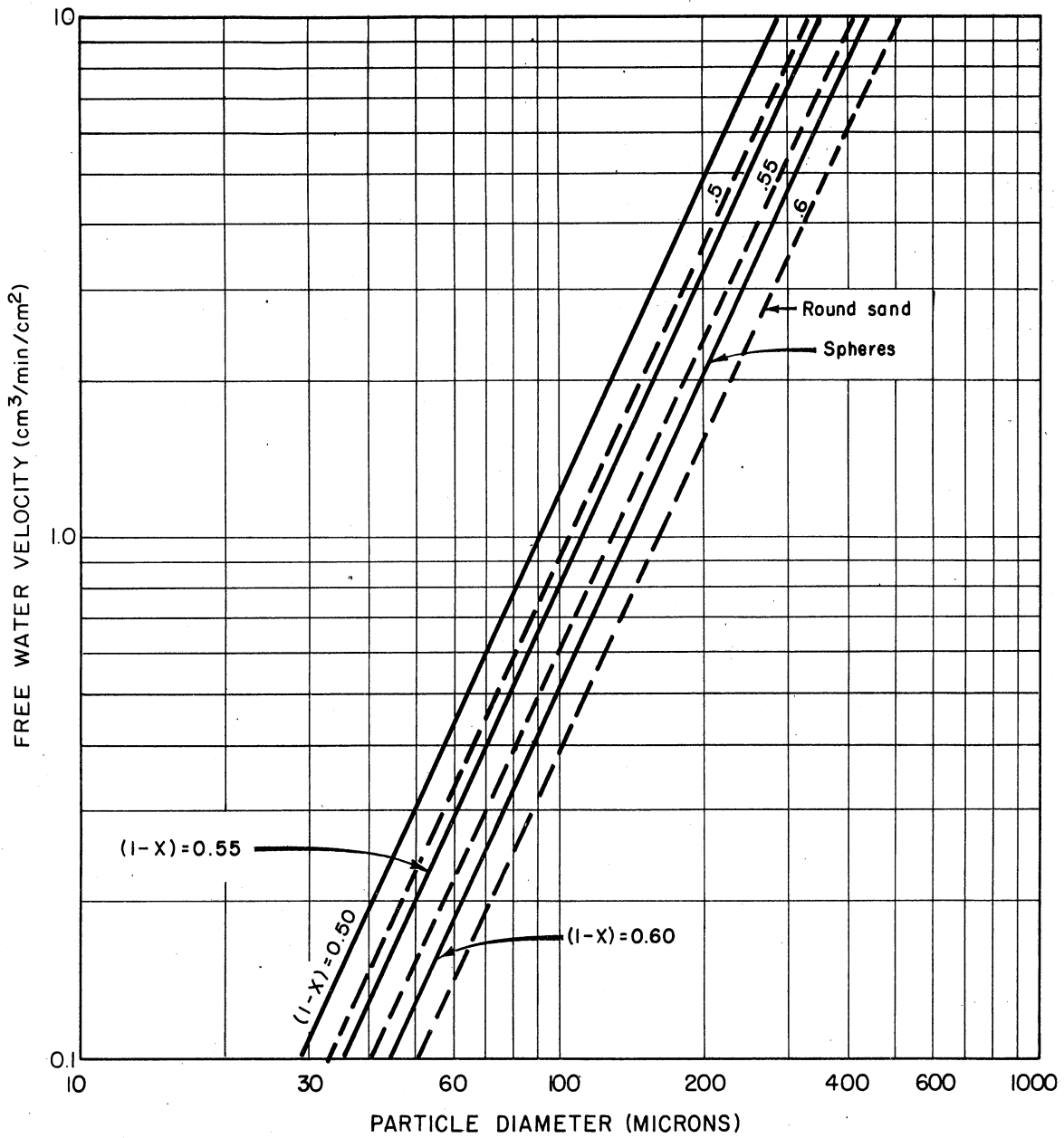


Fig. 20. Predicted free water velocity versus particle diameter with volume fraction solids as parameter for spheres and "round sand" with density of 2.65 gm/cm³ flowing upward at $R_{ow} = 1$.

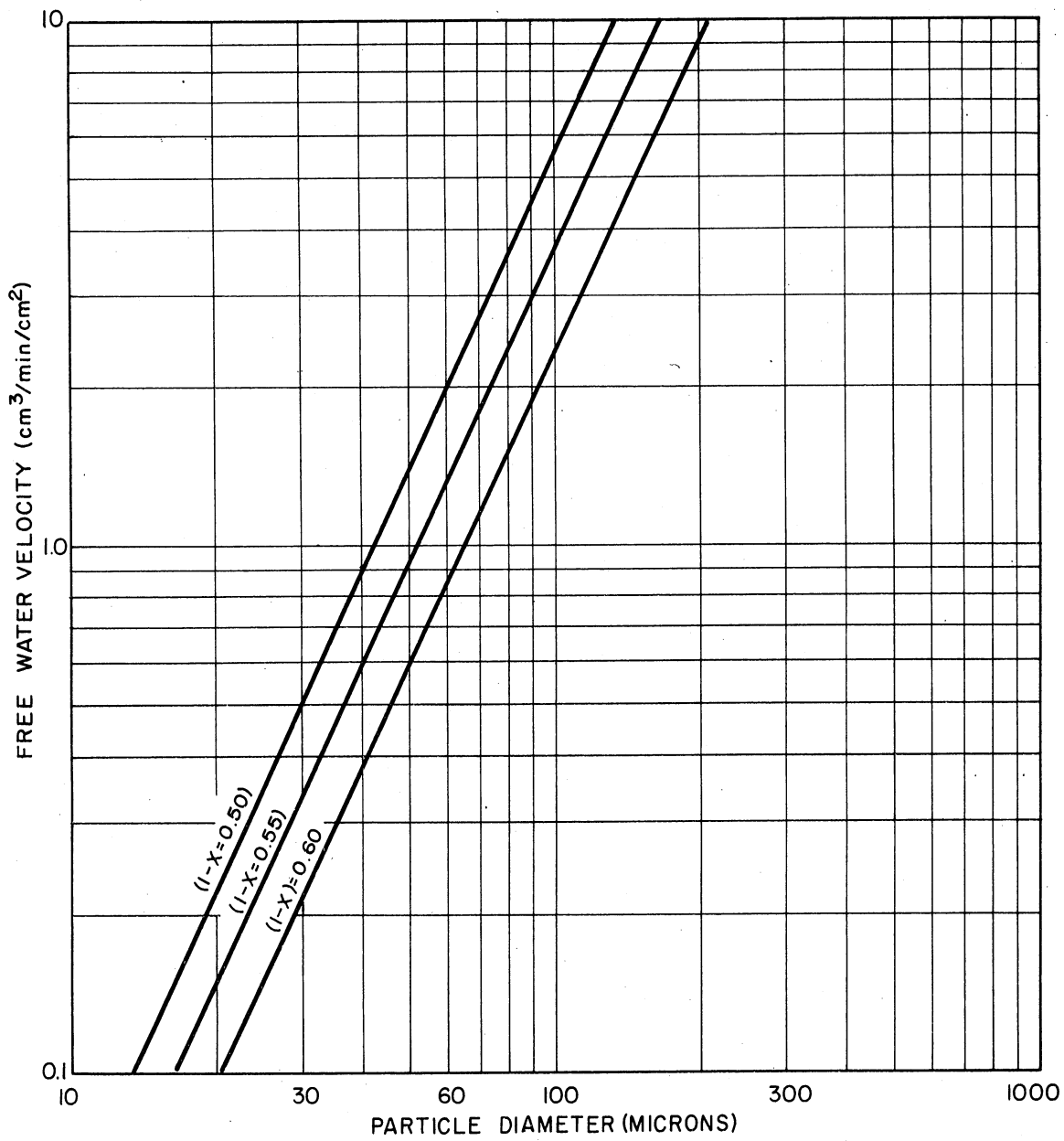


Fig. 21. Predicted free water velocity versus particle diameter with volume fraction solids as parameter for spheres with density of 8.65 flowing upward at $R_{ow} = 1$.

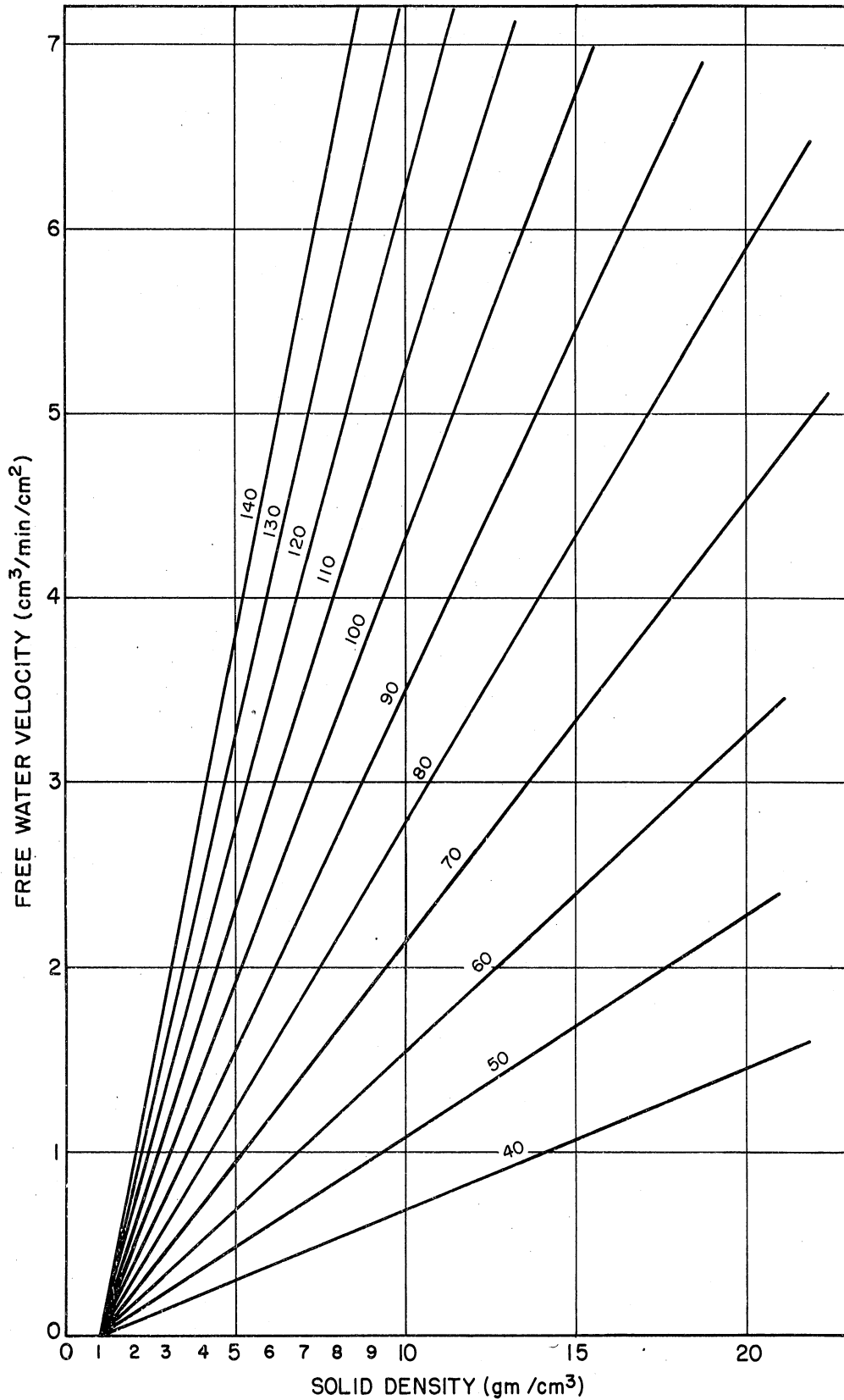


Fig. 22. Predicted free water velocity versus particle density with particle diameter as parameter for upward flow of spheres at $R_{ow} = 1$ and $(1-X) = 0.55$.

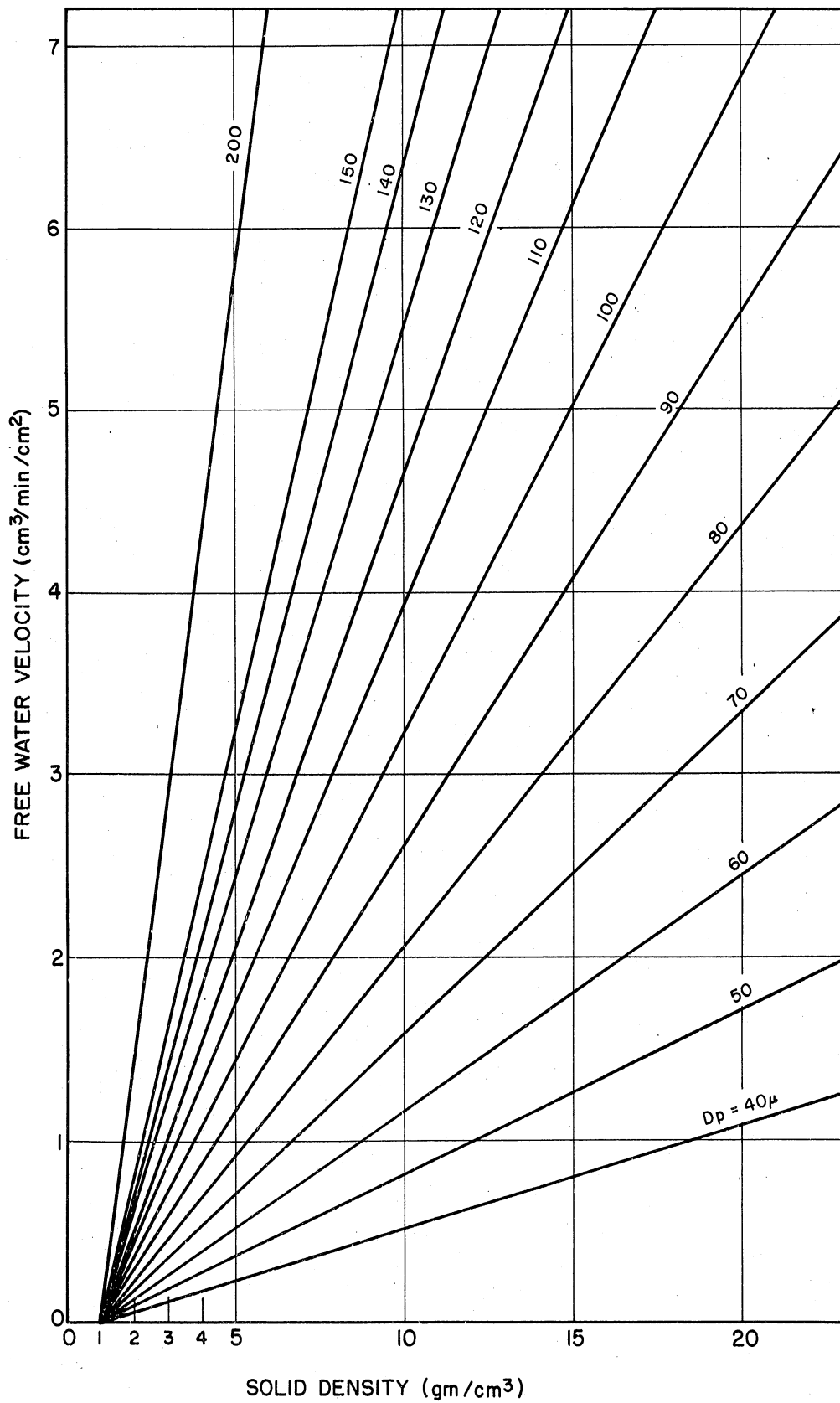


Fig. 23. Predicted free water velocity versus particle density with particle diameter as parameter for upward flow of "round sand" at $R_{ow} = 1$ and $(1-X) = 0.55$.

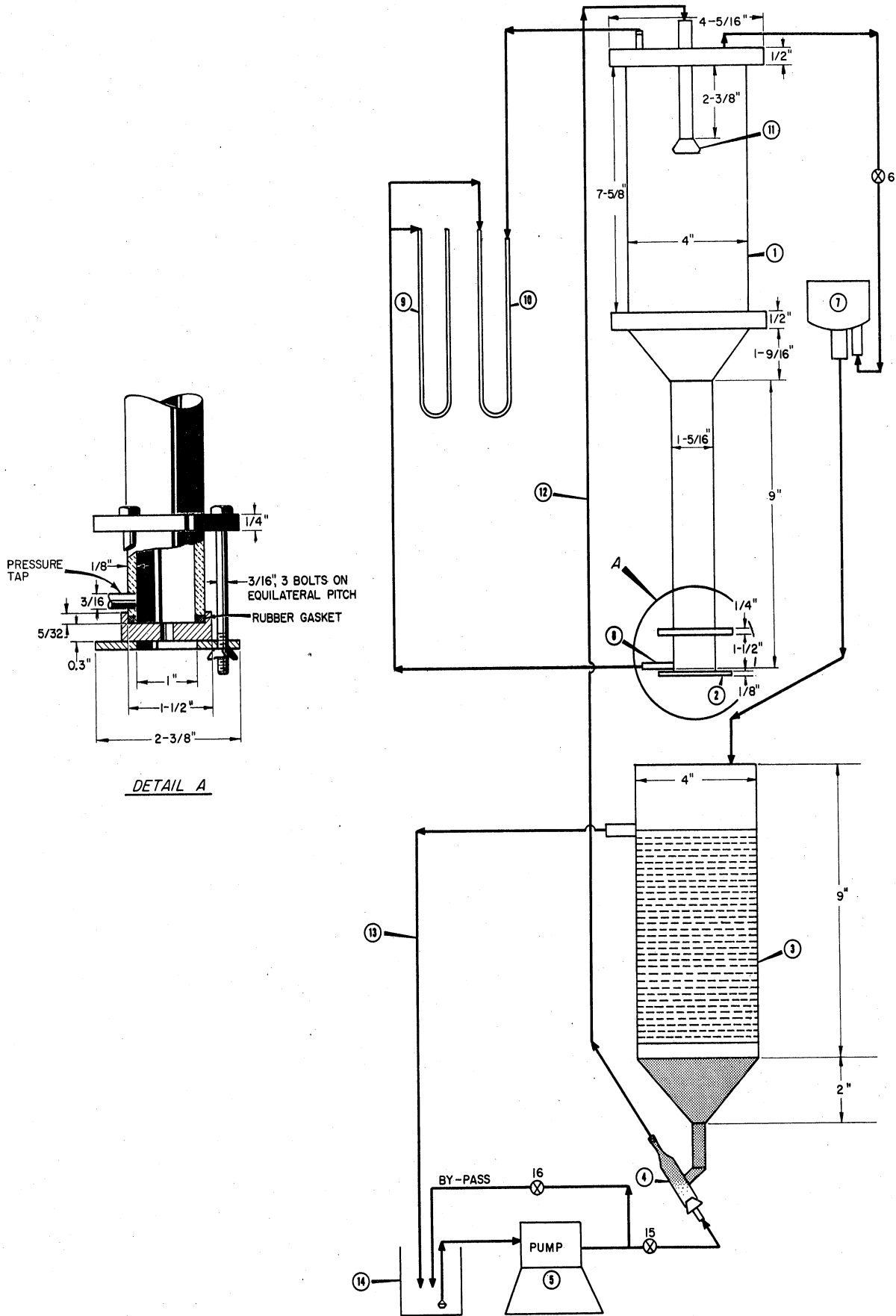


Fig. 24. Sketch of equipment.

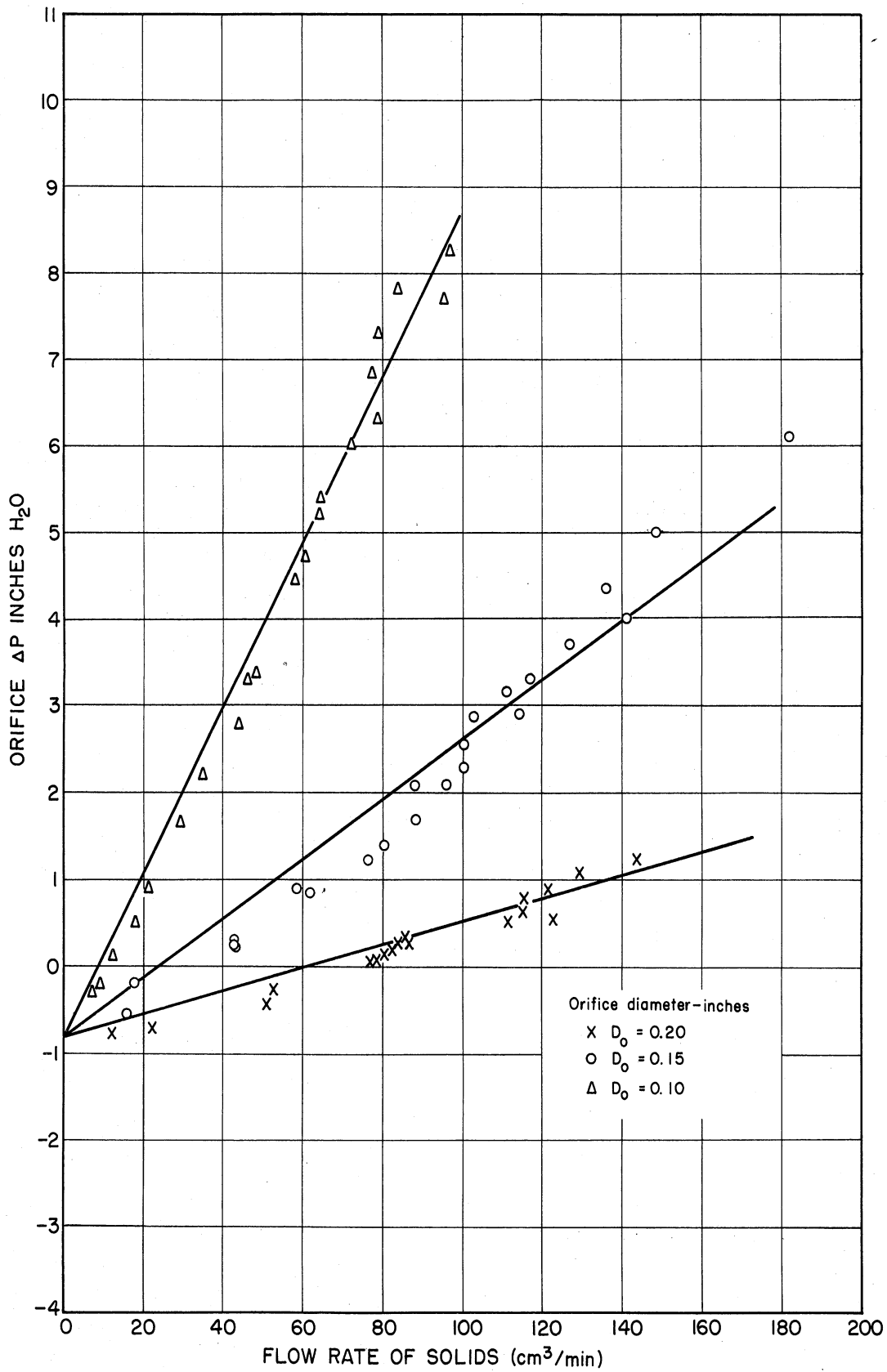


Fig. 25. Pressure drop versus solids flow rate with orifice diameter as parameter for the flow of 80/100-mesh Ottawa sand paste.

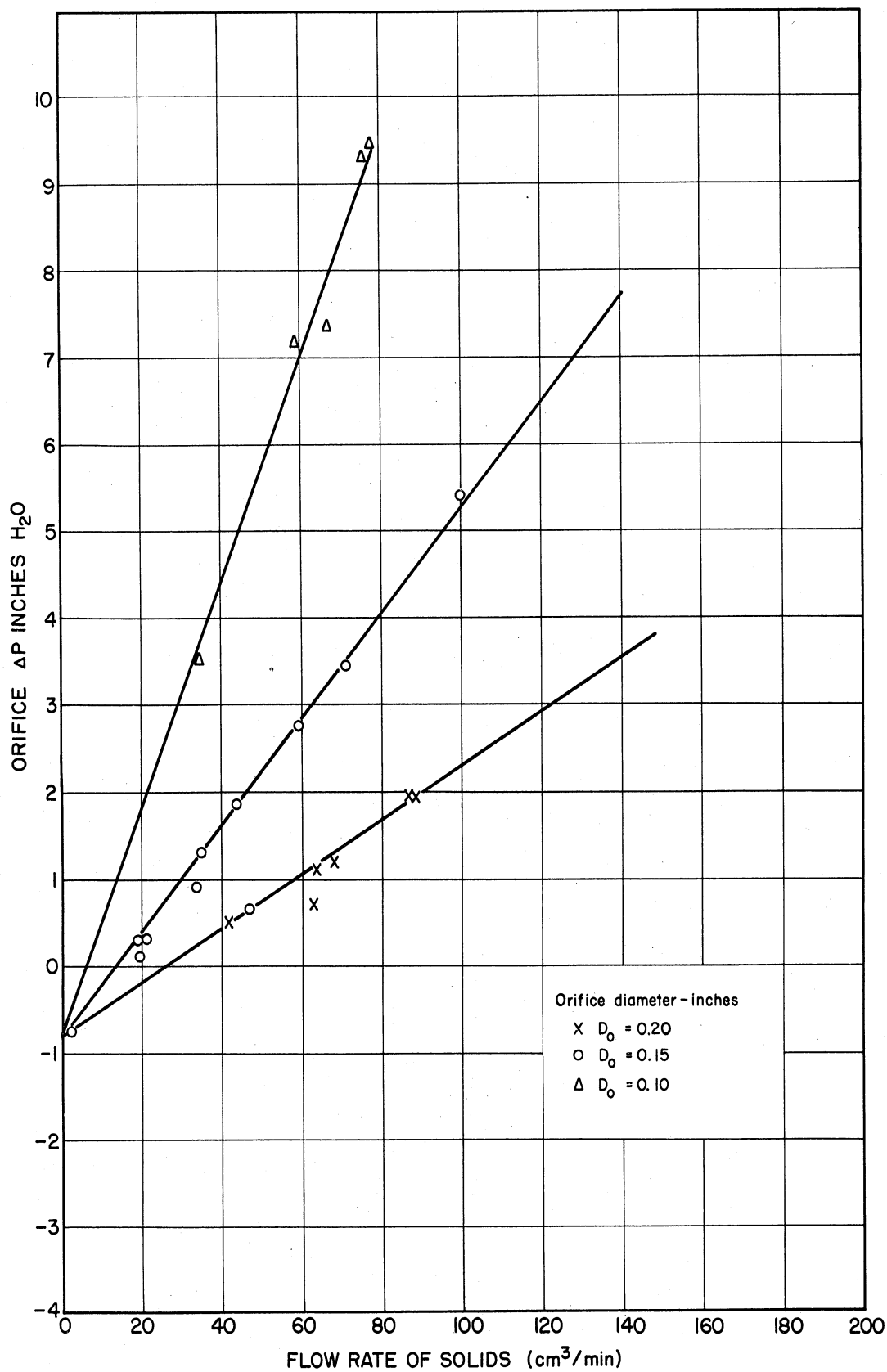


Fig. 26. Pressure drop versus solids flow rate with orifice diameter as parameter for the flow of 140/200-mesh Ottawa sand paste.

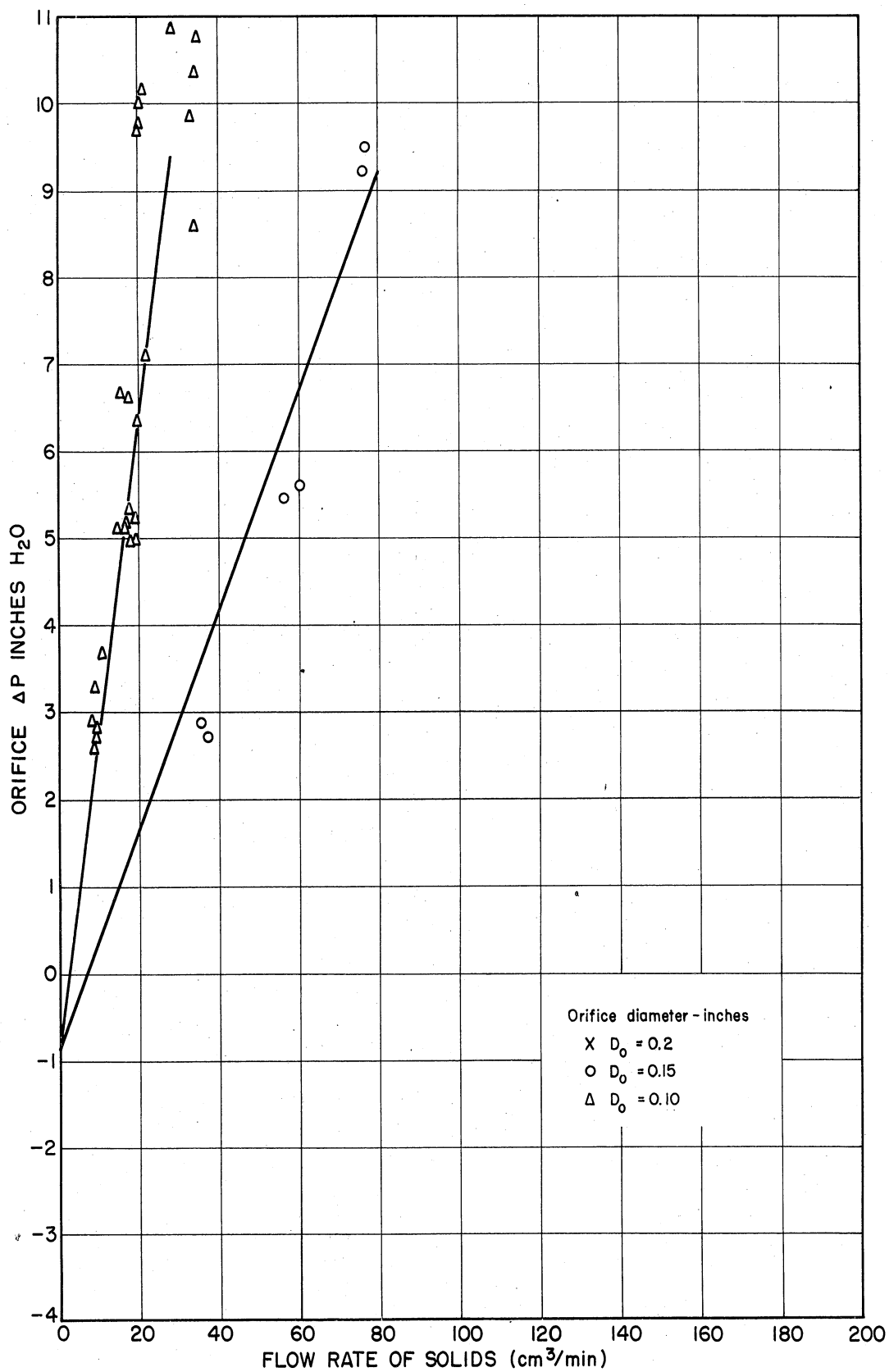


Fig. 27. Pressure drop versus solids flow rate with orifice diameter as parameter for the flow of 200/325-mesh Ottawa sand paste.

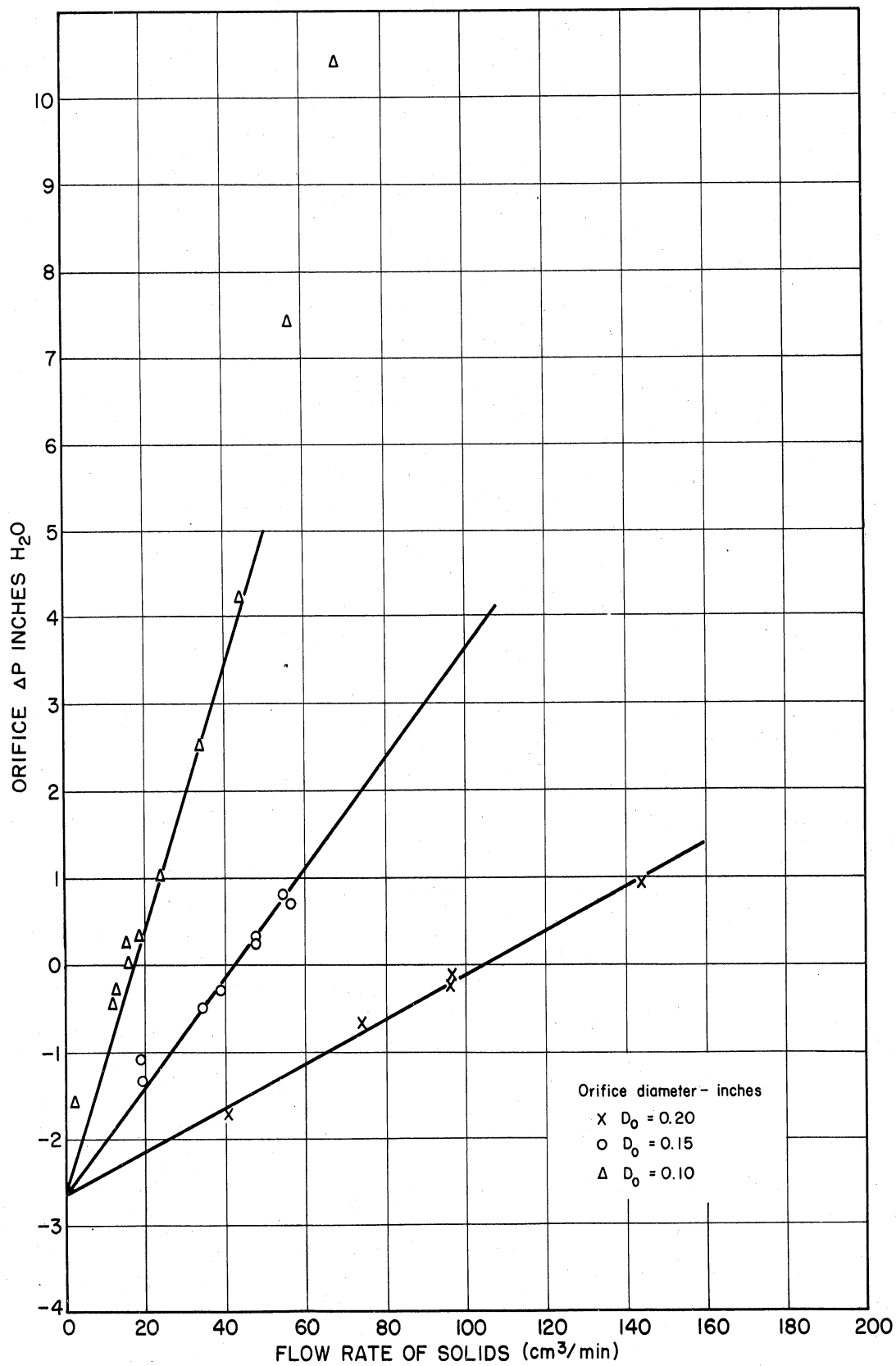


Fig. 28. Pressure drop versus solids flow rate with orifice diameter as parameter for the flow of 140/200-mesh copper shot.

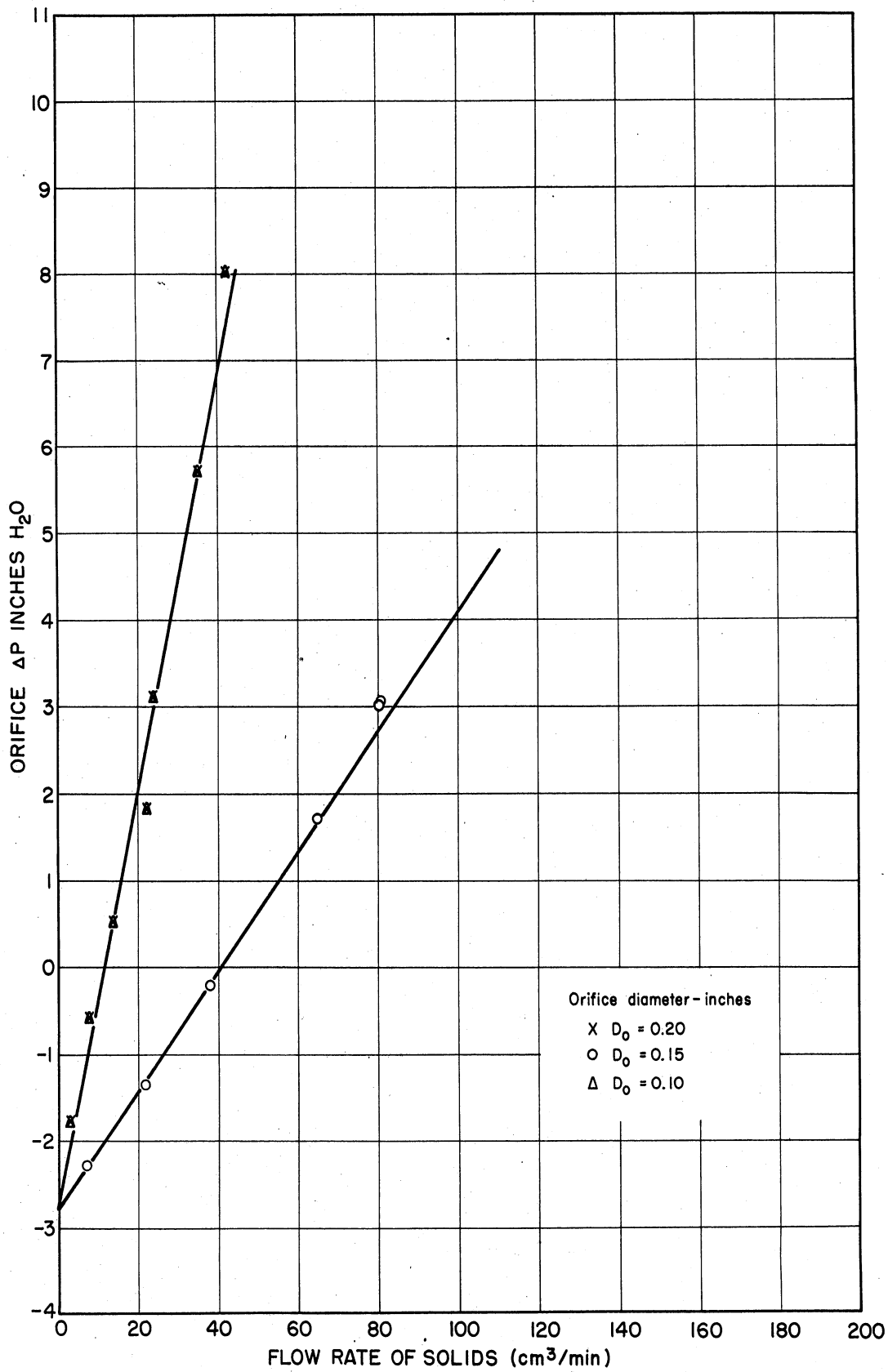


Fig. 29. Pressure drop versus solids flow rate with orifice diameter as parameter for the flow of 140/200-mesh lead shot.

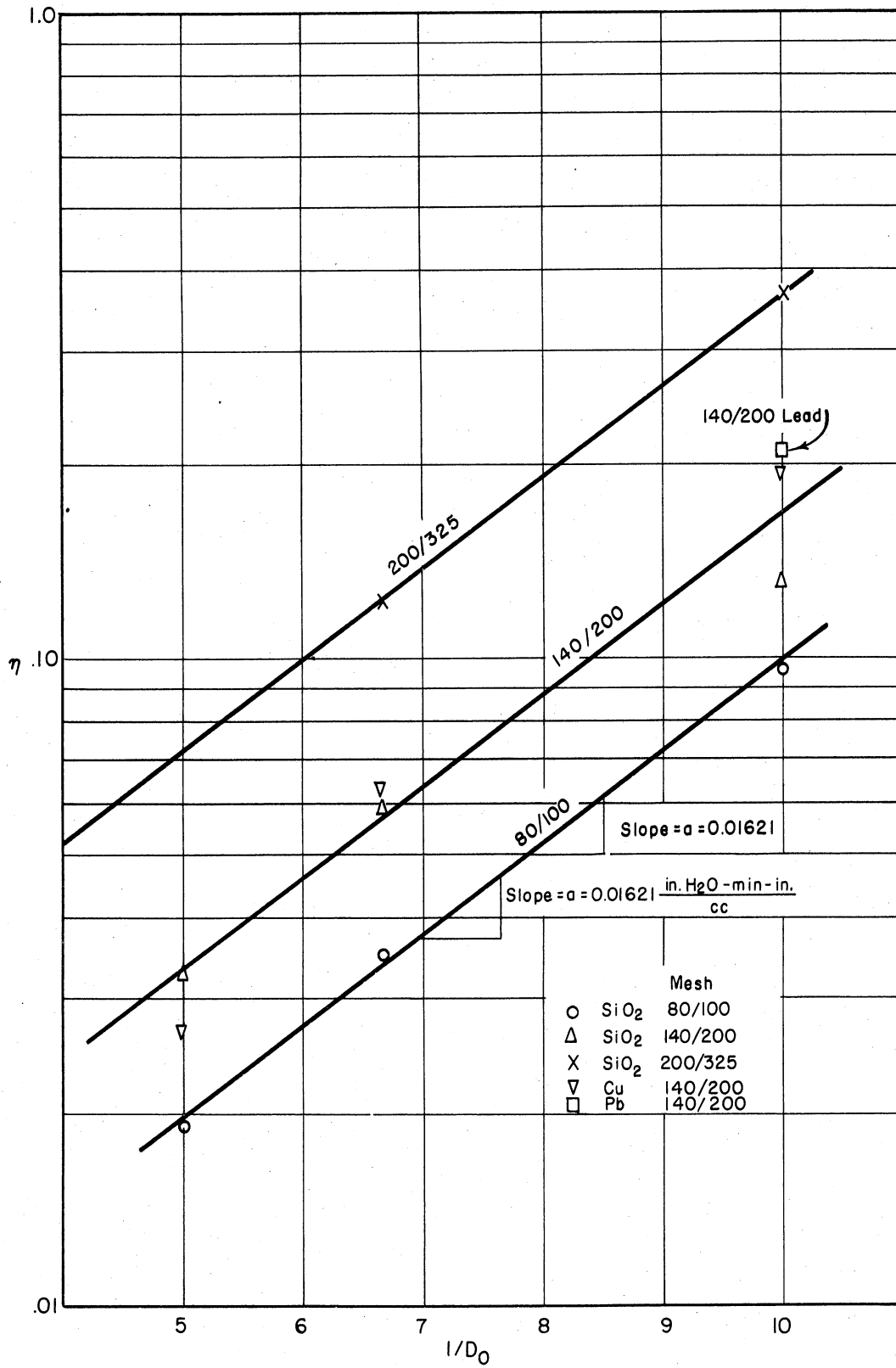


Fig. 30. Logarithm of the slope function versus reciprocal of orifice diameter.

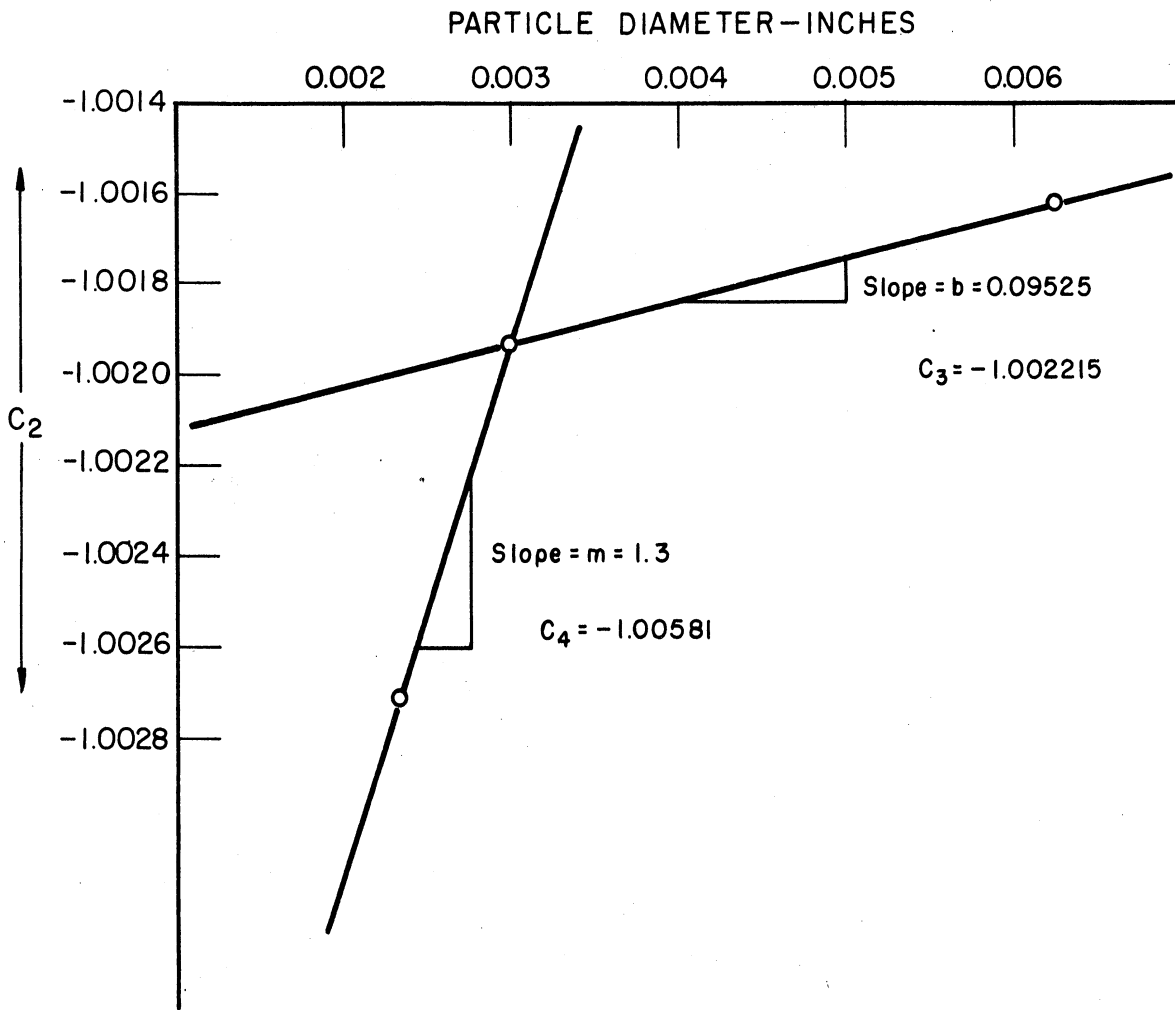


Fig. 31. C_2 versus particle diameter.

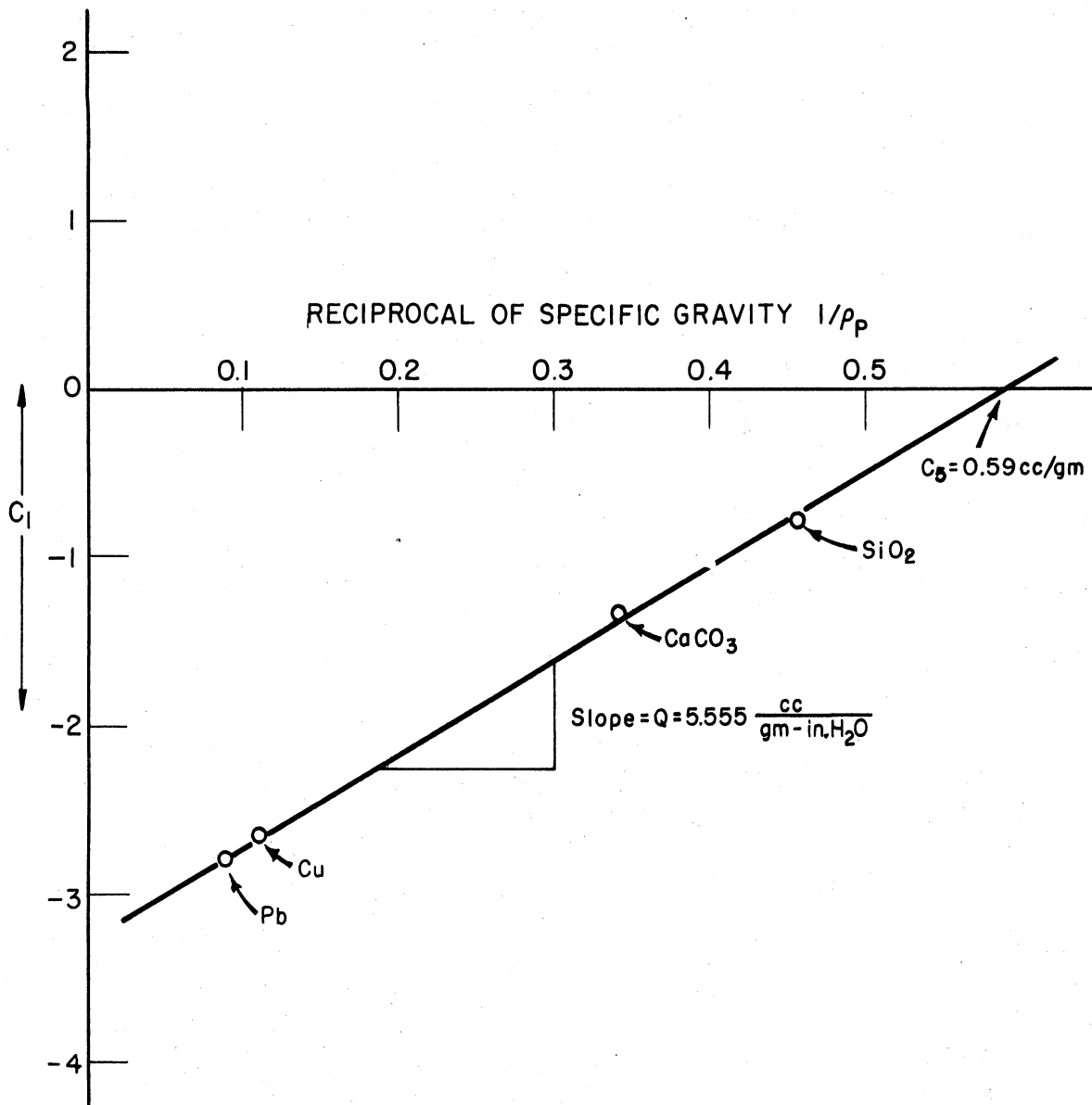


Fig. 32. C_1 versus reciprocal of particle density.

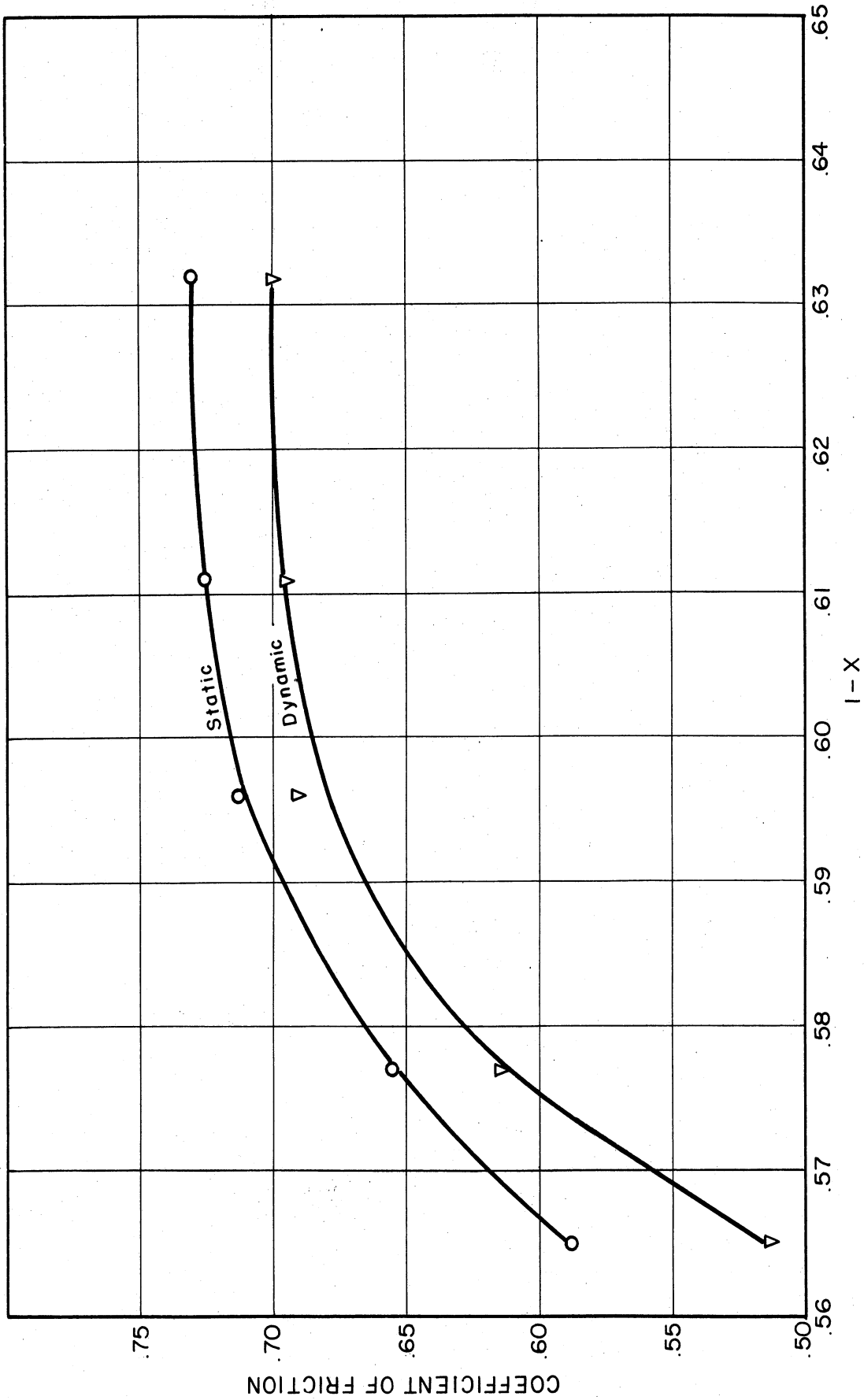


Fig. 33. Coefficient of friction between a zinc plate and 150/200-mesh Ottawa sand paste.

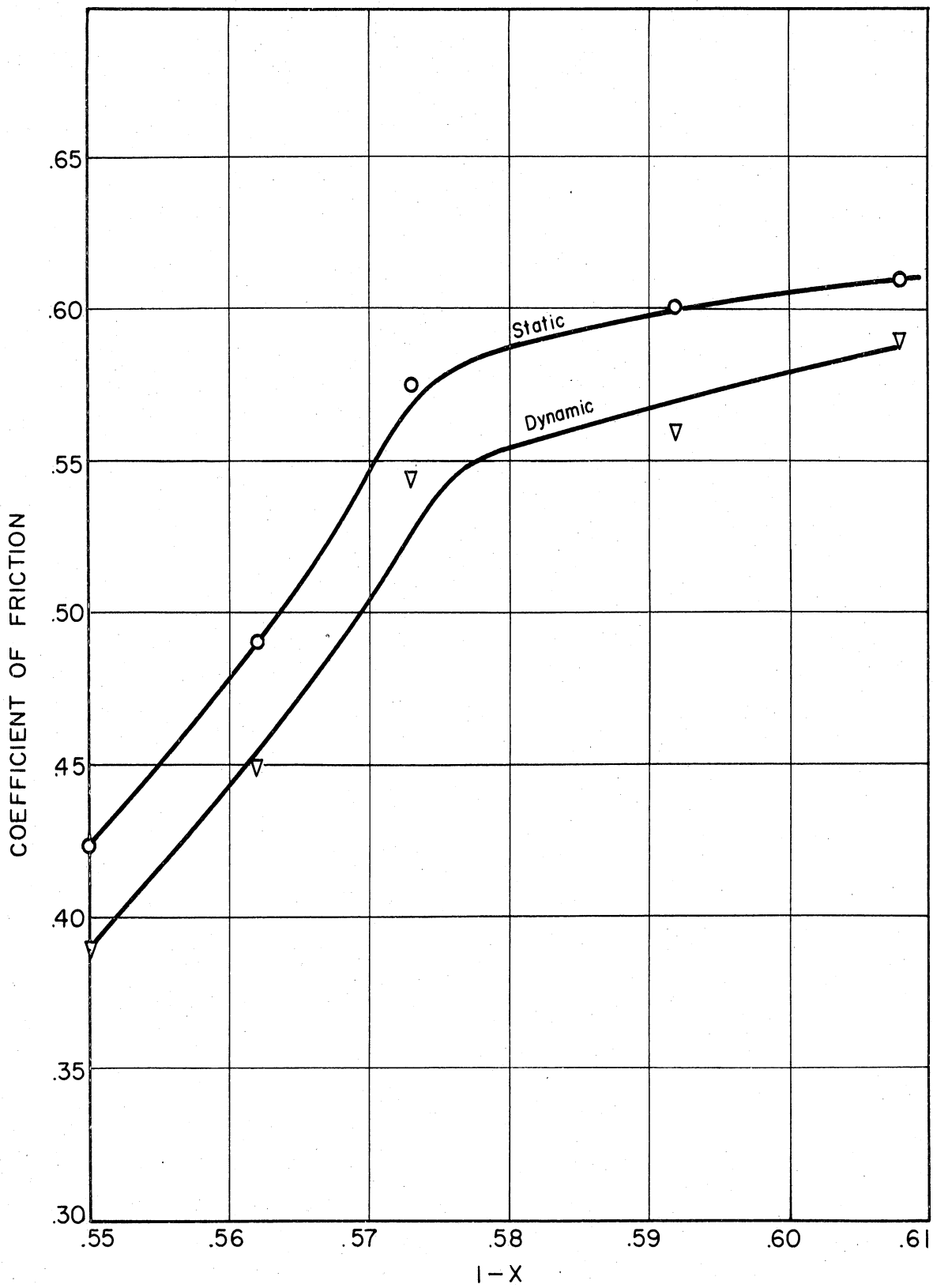


Fig. 34. Coefficient of friction between a glass plate and 150/200-mesh Ottawa sand paste.

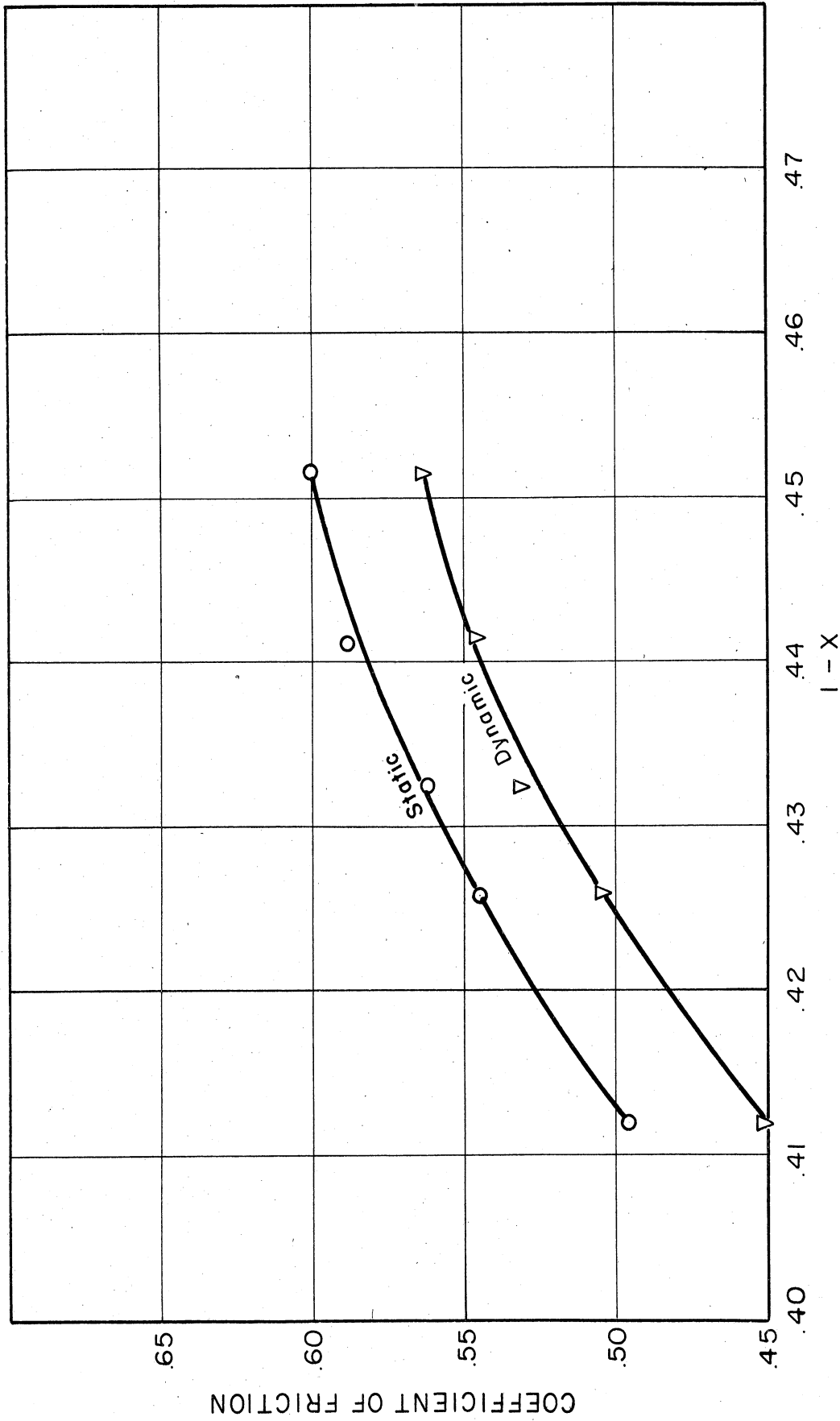


Fig. 35. Coefficient of friction between a glass plate and -325-mesh iron-powder paste.

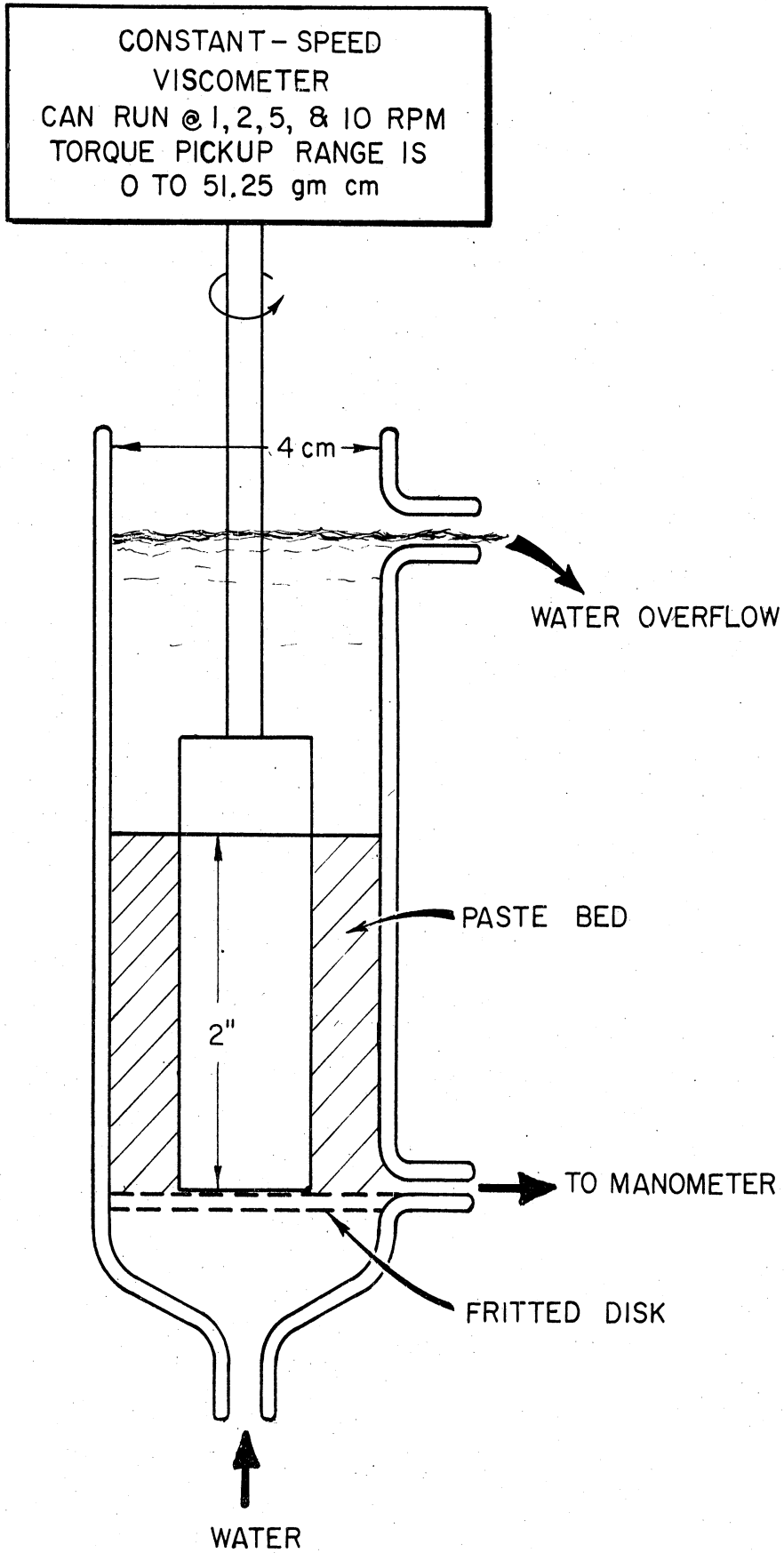


Fig. 36. Viscometer apparatus sketch.

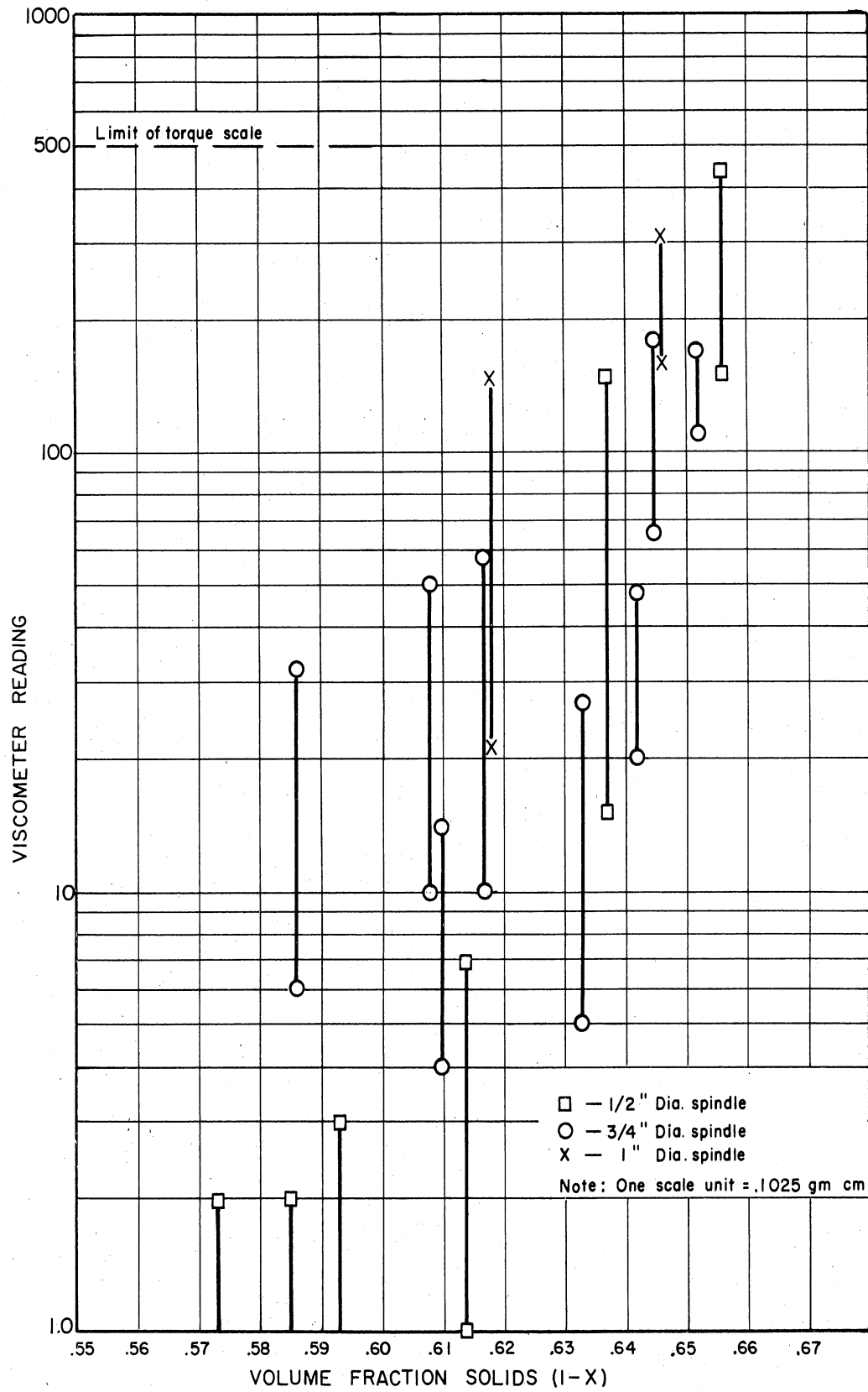


Fig. 37. Viscometer torque versus fraction solids for 100/140-mesh Ottawa sand.

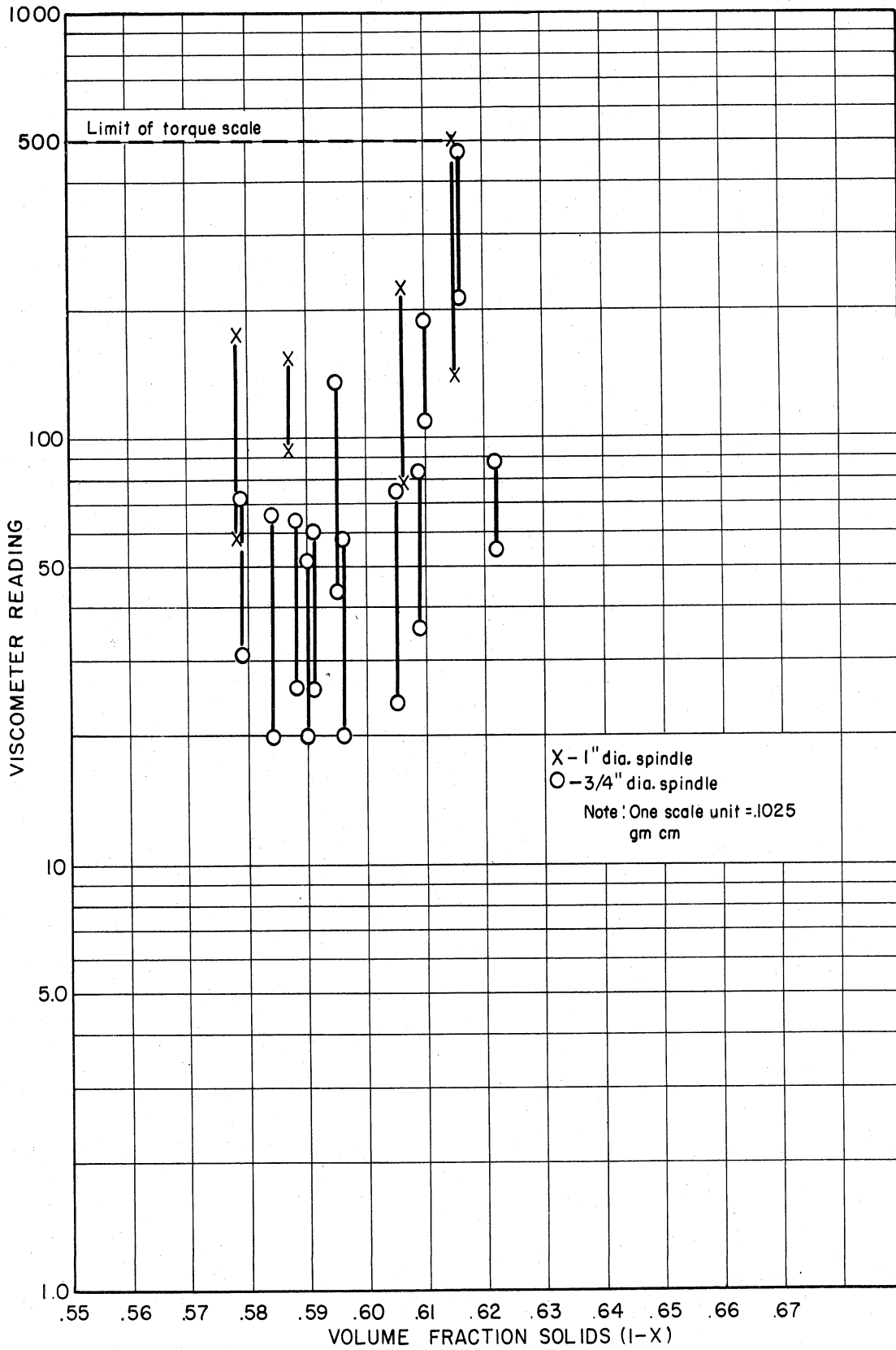


Fig. 38. Viscometer torque versus fraction solids for 100/140-mesh copper shot.

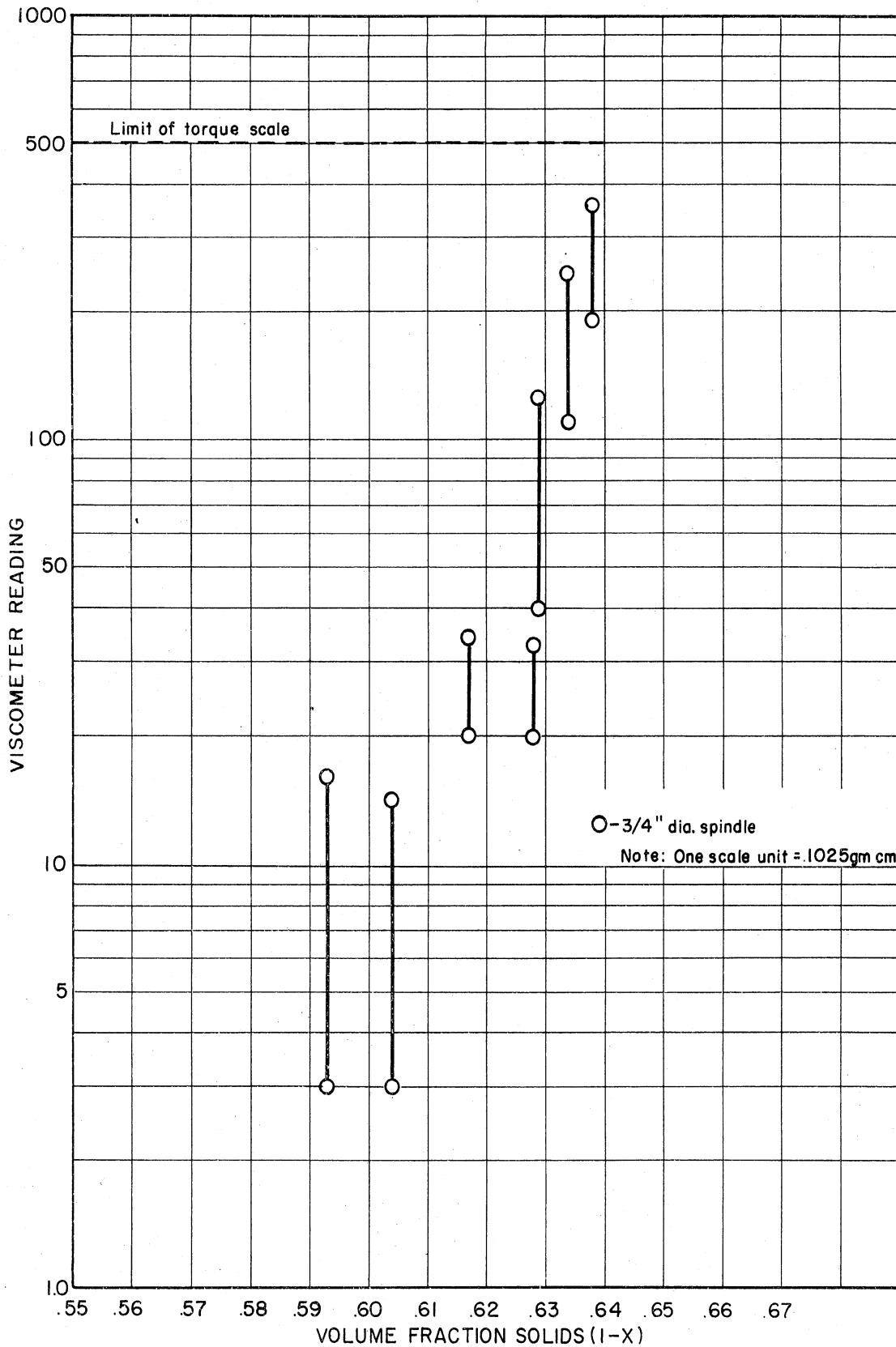


Fig. 39. Viscometer torque versus fraction solids for 100/120-mesh glass beads.

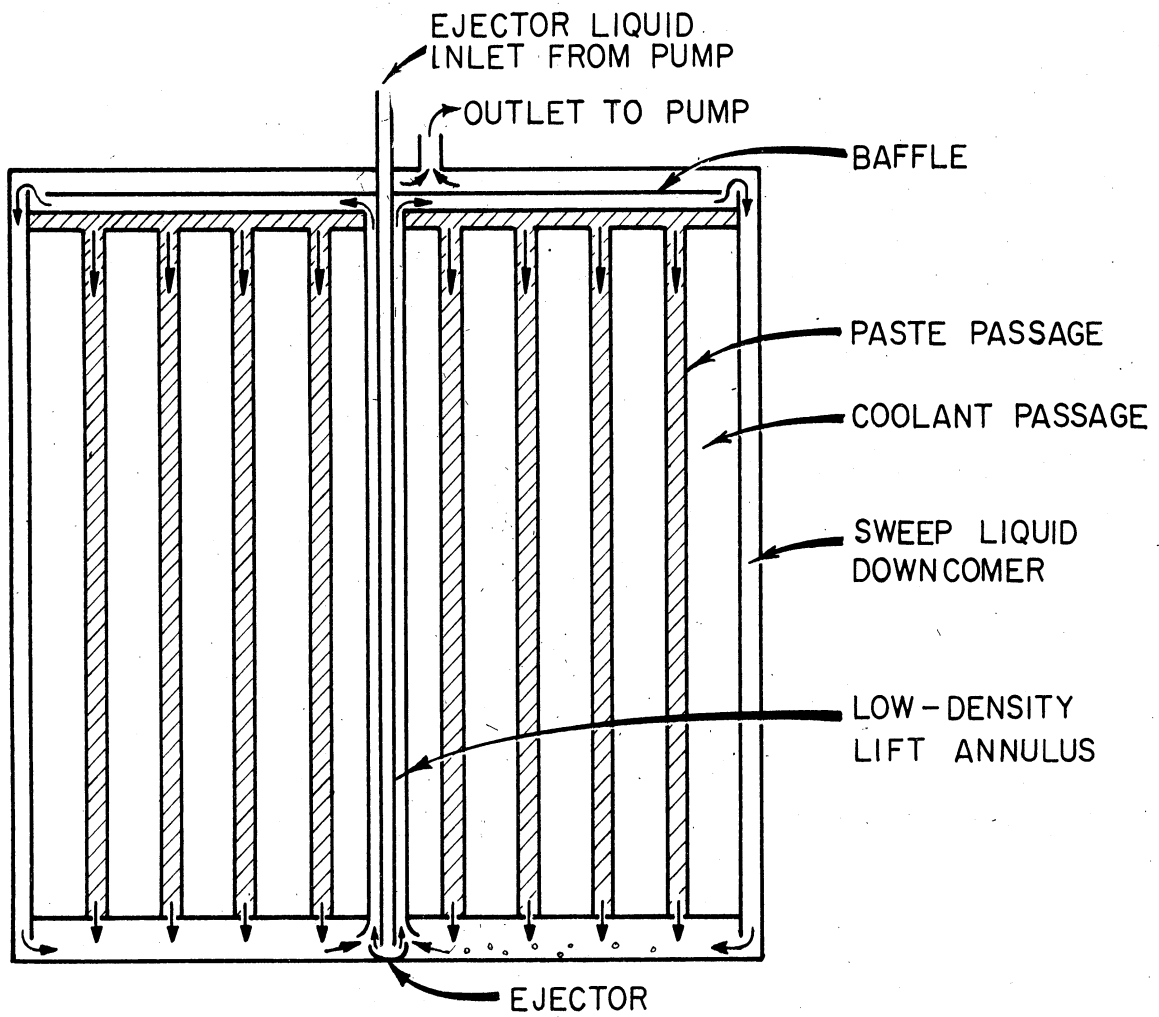


Fig. 40a. Complete reactor configuration.

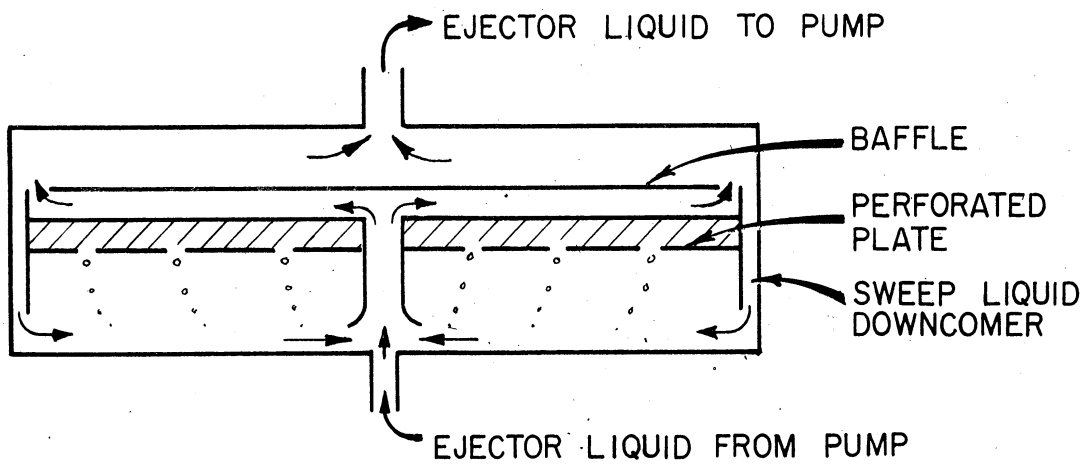


Fig. 40b. Experimental model configuration.

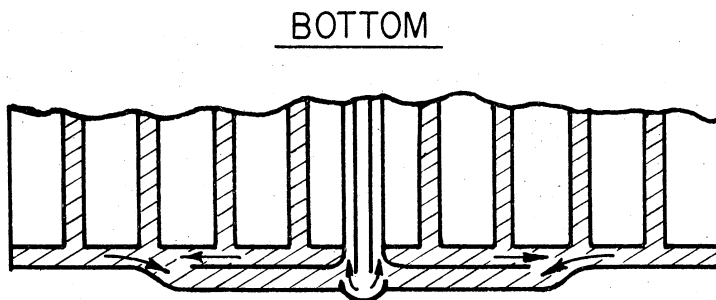
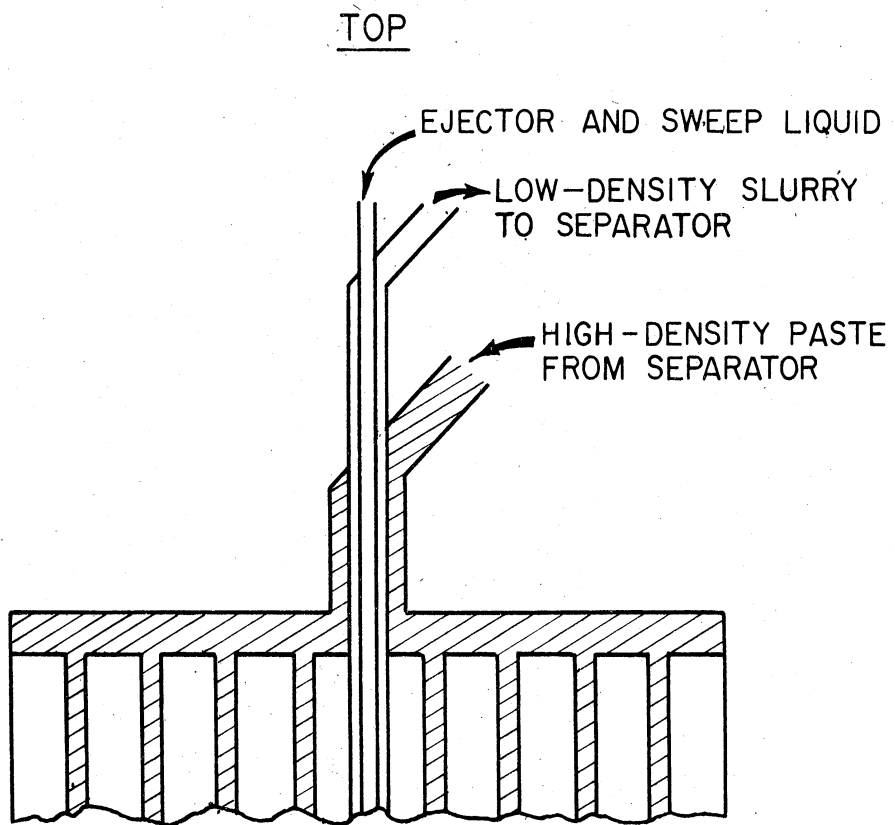


Fig. 41. Reactor top and bottom configurations.



3 9015 02651 5323